THE ESTIMATION OF THE PARTICLE SIZE OF RESPIRABLE CRYSTALLINE SILICA (PSD_{RCS}) FROM THE PARTICLE SIZE DISTRIBUTION MEASUREMENT OF ARCHIVED DUST SAMPLES (PSD_{DUST})

Cecilia Johanna Pretorius

A Dissertation submitted to the Faculty of Health Sciences, University of the Witwatersrand, Johannesburg, in fulfilment of the requirements for the degree of Master of Science in Medicine (Exposure Science)

March 2025 (Revision 2)

Declaration

I, Cecilia Johanna Pretorius, declare that this Dissertation is my own, unaided work. It is being submitted for the Degree of Master of Science in Medicine (Exposure Science), at the University of the Witwatersrand, Johannesburg. It has not been submitted before for any degree or examination at any other University.

Cecilia Johanna Pretorius

Signed on the 10th day of March 2025 in Pretoria

Abstract

Max 250 words

The study aimed to investigate the performance of an affordable, high-throughput method, i.e. Laser Light Scattering (LLS) to estimate the particle size of respirable crystalline silica (RCS) in archived dust samples, by comparing the results obtained by LLS with the results from a Scanning Electron Microscopy (SEM), the gold standard, an expensive, labour-intensive method. The length and width of approximately 100 RCS particles were measured using SEM (SEM_{RCS}) in 12 respirable dust samples from NIST, Arizona dust and gold mine dust. The remainder of the dust sample was used to measure the particle size distribution (PSD) of all the dust particles using LLS (LLS_{Dust}). Linear regression models were derived for SEM_{RCS} and LLS_{Dust} pairs, i.e., volume, length and area, and these regression models were used to estimate the SEM_{RCS} from the LLS_{Dust}. The estimated SEM_{RCS} was compared with the measured SEM_{RCS}, and it was found that LLS_{Dust} is not a good predictor of SEM_{RCS} and future research is needed to explore whether a more robust prediction model can be developed. In this study it was found that improvements on the SEM_{RCS} methodology can be made to make the measurements more efficient and affordable. Hence, since a better estimate of the PSD of RCS will improve both the risk assessment and measures to control RCS in workplaces, it is recommended that direct SEM measurements of the RCS particle size are routinely incorporated.

231 words

Keywords: laser light scattering (LLS), respirable crystalline silica, scanning electron microscopy (SEM), particle size

Acknowledgements

The author wishes to thank the following individuals and organisations:

1. Prof. Derk Brouwer and Prof. Jill Murray for their guidance, support and patience throughout their supervision.
2. Prof. Elena Libhaber and Mr. Anteneh Yalew for their assistance and guidance with the statistical analysis.
3. Mr. Kevin Beaumont for his editorial guidance and support.
4. The National Metrology Institute of South Africa (NMISA) for making the Scanning Electron Microscope (SEM) available for the analysis of the samples and, specifically, Mrs. Loukie Adlem for her technical advice and support.
5. The Council for Scientific and Industrial Research’s (CSIR) Air and Dust Laboratory for allowing the use of archived samples, and for making the Laser Light Scattering instrument available for my analysis.

To my family, Christoff, Gerber and CJ – I love you with all my heart!

Praise the Lord for his unfailing love! “Truly He is my rock and my salvation; He is my fortress; I will never be shaken.” Psalms 62:2

Table of Contents

List of Figures

List of Tables

Glossary of Terms

In the context of this study, the following terms are explained:

Archived dust samples	Respirable dust samples that have been sent to the laboratory for analysis of respirable crystalline silica (RCS) mass and subsequently archived. For the purpose of this study, these archived samples are secondary samples.
Arizona dust	A standard test dust (ISO 12103-1) that consists of silica particles in a mineral matrix (i.e. RCS and non-RCS particles) and that has a known particle size distribution (PSD) as per the certificate of analysis from the supplier
D10	10% cumulative particle size, where 10% of the particles have a size distribution of below this value in micron (µm)
D30	30% cumulative particle size, where 30% of the particles have a size distribution of below this value in micron (µm)
D50 (median PSD)	50% cumulative particle size, where 50% of the particles have a size distribution of below this value in micron (µm)
D70	70% cumulative particle size, where 70% of the particles have a size distribution of below this value in micron (µm)
D90	90% cumulative particle size, where 90% of the particles have a size distribution of below this value in micron (µm)
Dust	The fine, dry powder that consists of all particles of a material (respirable crystalline silica (RCS) and non-RCS). The dust types in the different respirable dust samples for this study are NIST (pure RCS), Arizona (RCS and non-RCS) and gold mine dust (RCS and non-RCS).
Gold mine dust	Respirable dust samples from a South African gold mine with RCS particles in an unknown mineral matrix (i.e. non-RCS particles) with an unknown PSD
Known dust	The elemental composition and PSD of this dust are known; i.e. either a certificate or material safety data sheet (MSDS) is available.
Laser Light Scattering (LLS)	An analytical test method that uses the diffraction of a laser beam by dust particles to calculate the size distribution of particles. The size distribution calculated in this way is expressed as $PSD_{LLS(Dust)}$.
Mineral matrix	The composition of the dust material that consists of components from geological minerals.
NIST dust	Standard Reference Material that consists of pure silica (SiO_2) with a known composition and particle size distribution as per the certificate of

	analysis from the supplier, the National Institute of Standards and Technology (NIST)
Non-RCS	Dust particles with a elemental composition other than respirable crystalline silica, such as alumina-silicates that are found in mine dust.
Particle size distribution (PSD)	The size distribution of dust particles that are between one and ten micron (µm) and expressed in terms of the PSD parameters D10, D30, D50, D70 and D90 (µm)
PSD metric	The measurand for the particle size method. Different PSD metrics were obtained from each PSD method
SEM	length, cross-sectional diameter (dc), spherical diameter (ds) and spherical volume (V)
LLS	Volume, Area, Length and Number
Particle	The smallest unit or building block of dust
RCS concentration	The mass (in mg) of respirable crystalline silica in a volume (in m^3) of air
RCS mass	Mass (in mg) of respirable crystalline silica as measured in the laboratory using X-ray Diffraction (XRD)
Refractive index	A ratio of how the laser light is scattered by a material in a vacuum versus in a watery medium
Respirable Crystalline Silica (RCS)	Crystalline particles with an elemental composition of silicon dioxide and with an approximate size range of less than ten micron (depending on the performance of the sampling equipment)
Respirable fraction	According to ISO 7708 (ISO, 1995), the respirable fraction is the mass fraction of total airborne particles that penetrates the unciliated airways. Sampling equipment selects the size fraction of particles that are approximately less than ten micron. Depending on the performance of the sampling equipment and the nature of the material sampled, this range does not exclude particles larger than ten micron
Respirable dust sample	A filter membrane (25 mm in diameter) with a deposition of dust that has been captured from air with an efficacy similar to the respirable convention (ISO, 1995). In general, particles with an aerodynamic diameter of less than ten micron are captured. As stated in “Respirable fraction”, particles smaller than one micron may also be captured with high efficiency. The sample is submitted to the laboratory for RCS analysis using XRD and is archived afterwards
Sample	In this study a sample is an item that is analysed, i.e. the respirable dust sample

Scanning Electron Microscopy (SEM)	An analytical test method that uses charged electrons to generate an image of individual dust particles. From this image, the size of the dust particles can be measured using the software, ImageJ. Expressed as $PSD_{SEM(Dust)}$
SEM Energy Dispersive X-rays Spectroscopy (SEM-EDX or SEM-EDS)	In addition to SEM, the EDX (also known as EDS) uses X-rays to determine the elemental composition of an individual dust particle. Expressed as $PSD_{SEM(RCS)}$
Silica	Dust particles with a elemental composition of silicon dioxide (SiO_2).

List of Abbreviations, Acronyms and Symbols

µm	micron
2D	two-dimensional
3D	three-dimensional
A&D	Air and Dust
Al	Aluminium
BIPM	International Bureau for Weights and Measures
CIPM	International Committee for Weights and Measures
CoA	Certificate of Analysis
CSIR	Council for Scientific and Industrial Research
D10	10% cumulative particle size distribution
D30	30% cumulative particle size distribution
D50	50% cumulative particle size distribution
D70	70% cumulative particle size distribution
D90	90% cumulative particle size distribution
DMRE	Department of Mineral Resources and Energy
DoEL	Department of Employment and Labour
dc	cross-sectional diameter
ds	spherical diameter
EDS	Energy Dispersive Spectroscopy
EDX	Energy Dispersive X-rays
eV	electron volts
FTIR	Fourier-Transform Infrared
IARC	International Agency for Research on Cancer
ISO	International Organization for Standardization
ILO	International Labour Organisation
keV	kilo electron volts
LLS	Laser Light Scattering
mbar	millibar
MHSI	Mine Health and Safety Inspectorate
MSDS	Material Safety Data Sheet
m^3	cubic metre

mg	milligram
NIH	National Institute of Health
NIOSH	National Institute of Occupational Safety and Health
NIST	National Institute for Standards and Technology
NMISA	National Metrology Institute of South Africa
NPES	National Programme for the Elimination of Silicosis
OEL	Occupational Exposure Limit
PSD	Particle Size Distribution
PSD_{Dust}	Particle Size Distribution of respirable dust
$PSD_{LLS(Dust)}$	Particle Size Distribution of all the particles that the dust is comprised of, as measured using LLS
PSD_{RCS}	Particle Size Distribution of Respirable Crystalline Silica
$PSD_{SEM(Dust)}$	Particle Size Distribution of dust as measured using SEM
$PSD_{SEM(RCS)}$	Particle Size Distribution of RCS as measured using SEM
RCS	Respirable Crystalline Silica
SA	South Africa
SANAS	South African National Accreditation System
SANS	South African National Standard
SEM	Scanning Electron Microscopy
SEM dc	cross-sectional diameter as determined by SEM
SEM ds	spherical diameter as determined by SEM
SEM V	volume as determined by SEM
Si	Silicon
SiO_2	Silica
SOP	Standard Operating Procedure
SRM	Standard Reference Material
Vol	volume
XRD	X-Ray Diffraction

Executive Summary

Despite efforts to eliminate workplace exposure to respirable crystalline silica (RCS) and reduce the incidence of silicosis, at least 200 new cases of silicosis are reported annually in the South African mining industry. Particles in the size range of less than ten microns can enter the gas exchange regions of the lung and result in the onset of disease. Understanding the particle size distribution (PSD) of RCS will lead to improvements in RCS controls in workplaces and may result in a long-term reduction in the persistent prevalence of silicosis.

Although the RCS concentration as measured as mass concentrations, e.g. in mg/m3, remains the main focus of concern, other factors may contribute to the toxicity of RCS. The PSD of RCS has been implicated in the toxicity of RCS, but the size distribution of RCS in the airborne dust has not been fully explored. Laser Light Scattering (LLS) is a high-throughput and affordable method which determine the PSD of all dust particles in a respirable dust sample. Since LLS cannot discriminate particles with different compositions, the PSD of RCS particles within the respirable dust sample cannot be determined. Therefore, the present study aimed to determine if the PSD of all dust particles in a respirable dust sample, as measured by Laser Light Scattering (LLS), would be representative of the PSD of RCS in the same sample, as measured using Scanning Electron Microscopy (SEM). This study explored the PSD of RCS in archived respirable dust samples (NIST, Arizona and gold mine dust collected in a South African mine).

The objectives of the study were to:

To operationalise the Scanning Electron Microscopy (SEM) method for accuracy and the effort to measure particle size in respirable dust samples, through the accurate sizing of particles, with regard to the selection and the number of individual particles to be analysed in NIST, Arizona, and gold mine dust.

To compare the particle size distribution (PSD) attained by the Laser Light Scattering (LLS) method with the particle size distribution achieved by the Scanning Electron Microscopy (SEM) method and thus to show the relationship between the results obtained by the two methods, in NIST, Arizona and gold mine dust.

To estimate the particle size of respirable crystalline silica (RCS) from PSDLLS(Dust) and compare the estimated results with measured data (PSDSEM(RCS)) in NIST, Arizona and gold mine dust.

To operationalise the SEM method for RCS, a specimen was removed from the centre of the respirable dust sample. The length and width of approximately 100 individual RCS particles, in five different areas on the specimen, were measured on 12 samples from NIST, Arizona and gold mine dust. Although the ImageJ software on SEM can automatically measure all the dust particles, only the isolated RCS particles were manually measured. The SEM-EDS mapping of the particles according to the elemental composition allowed for the RCS particles to be easily identified and isolated, and the particle sizes were measured using the line tool. Additional size measurements of the RCS particles were mathematically derived from the length and width measurements, e.g., area (length × width), and volume (SEM Vol).

The remainder of the sample was used for the LLS measurement. The PSD of all the dust particles was expressed for three metrics, i.e., as a function of the volume (LLS Vol), length (LLS Length), and area (LLS Area) distribution.

The D50 of the RCS particle measurements were combined for SEM and LLS, respectively, and each of the two data sets was tested for normality using the Shapiro-Wilk Test. The LLS PSD data was not normally distributed ($p < 0.001$) but the SEM data was, with $p > 0.121$. The median values were compared using the Wilcoxon rank sum test, showing significant differences between the median values of LLS and SEM for all three PSD metrics ($p < 0.007$).

Regression models with the SEM PSD metric as a dependent variable were obtained for the same PSD metrics, and there was insufficient evidence to conclude that the underlying distribution was not normal ($p > 0.05$). Application of the regression analysis showed that the estimated SEM values for all three PSD metrics were significantly different from the actual SEM values. This means that LLS is not a good predictor of SEM_{RCS} and future research is needed to explore whether a more robust prediction model can be developed.

An unexpected finding was that the median D50-values of RCS particles (SEM_{RCS}) for all three PSD metrics were larger than the median D50-values of the dust particles (LLSDust) containing RCS and non-RCS particles in all the samples analysed. Further research is required to determine if this outcome will be the same on a larger sample size and in other mineral matrices.

A better understanding of the PSD of RCS may result in improved measures to control RCS in workplaces. Routine measurement of RCS particle size using SEM may provide insight into the efficiency of controls to reduce airborne RCS.

Chapter 1: Introduction

1.1 Introduction

The particle size of respirable crystalline silica (RCS) less than ten micron is a health concern for workers who are exposed to airborne silica, because RCS causes various forms of lung disease. This study explores one aspect related to RCS, namely the particle size distribution (PSD), to gain a better understanding of how the PSD of RCS compares with the PSD of typical, respirable dust that is inhaled by workers. When particles smaller than 2 µm deposit in the gas exchange region of the lungs, the body cannot easily remove these small, foreign particles (WHO, 1999).

The outcomes of this study may be used to improve RCS control measures to reduce workplace exposure in mining and non-mining industries and, ultimately, reduce lung disease related to RCS.

1.2 Background to the study

Crystalline silica was classified as a Group 1 human carcinogen in 1997 by the International Agency for Research on Cancer (IARC, 2012). Subsequent to this classification, the Global Elimination of Silicosis Programme was established in 2003 by the International Labour Organisation (ILO). South Africa established its own National Programme for the Elimination of Silicosis (NPES) in 2004, under the leadership of the Department of Employment and Labour (DoEL).

The DoEL does not report annually on the incidence of silicosis or exposure data of employees in the non-mining industries (Brouwer & Rees, 2020). Comprehensive information continues to be limited, unavailable or not reported. Some reports produced for the Department suggest

that approximately 15% of employees who were measured were exposed to RCS concentrations above the occupational exposure limit (OEL) of 0.1 mg/m^3 (Brouwer & Rees, 2020).

At the Mine Health and Safety Summit held in 2014, the tripartite leadership of government, the mining industry, and organised labour committed itself to achieving the milestone that, after December 2024, no new cases of silicosis will be reported by unexposed mine employees who entered the mining industry after 2008 (MHSC, 2014). Stakeholders in government, the mining industry, and organised labour have committed themselves to these programmes and focused efforts are being made to eliminate workplace exposure to RCS.

At the 2022 Mine Health and Safety Summit, it was reported that industry is showing 91.1% progress against the milestone that was set for RCS exposure (refer to Figure 1.1).

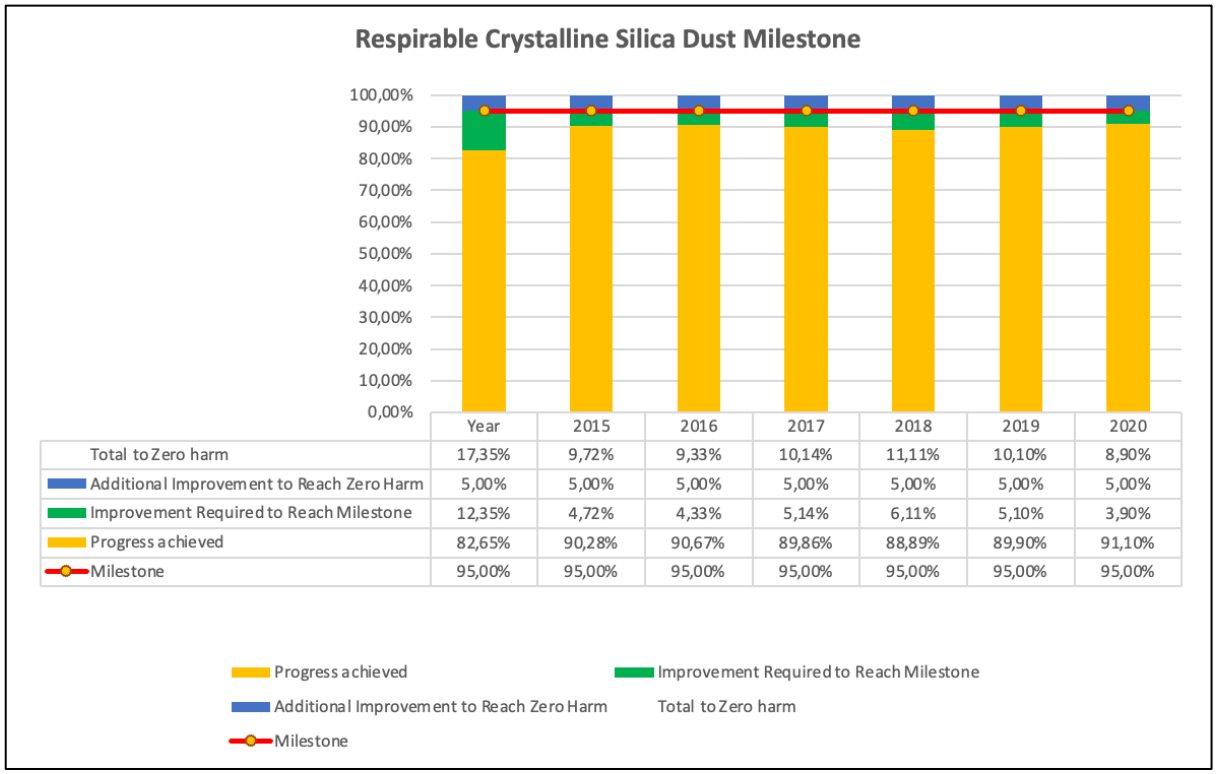

Year	2015	2016	2017	2018	2019	2020
Total to Zero harm	17,35%	9,72%	9,33%	10,14%	11,11%	10,10%	8,90%
Additional Improvement to Reach Zero Harm	5,00%	5,00%	5,00%	5,00%	5,00%	5,00%	5,00%
Improvement Required to Reach Milestone	12,35%	4,72%	4,33%	5,14%	6,11%	5,10%	3,90%
Progress achieved	82,65%	90,28%	90,67%	89,86%	88,89%	89,90%	91,10%
Milestone	95,00%	95,00%	95,00%	95,00%	95,00%	95,00%	95,00%

Figure 1.1: RCS exposure in the mining industry between 2015 and 2020 (Mamphitha, 2022)

Despite efforts to reduce worker exposure to the respirable fraction of crystalline silica since the start of the NPES and the implementation of the 2014 milestones, silicosis has not been eradicated. Although industry showed a decrease in silicosis cases between 2021 and 2022, there was still more than 200 cases of silicosis reported per annum according to the Mine Health and Safety Inspectorate's (MHSI) Annual Report of 2022/2023 (Figure 1.2; DMRE, 2023).

	SILICOSIS		PTB		SILICO-TUBERCULOSIS (Sil+TB)	
	2021	2022	2021	2022	2021	2022
Eastern Cape	0	0	1	3	0	0
Free State	78	116	160	167	1	15
Gauteng	68	56	102	122	6	3
KwaZulu-Natal	1	0	8	27	0	0
Limpopo	4	2	46	33	0	0
Mpumalanga	12	5	108	118	0	0
Northern Cape	0	5	10	17	0	0
North West: Klerksdorp	70	42	90	86	5	2
North West: Rustenburg	7	22	267	265	0	0
Western Cape	0	0	1	1	0	0
TOTAL	**240**	**248**	**793**	**839**	**12**	**20**

Figure 1.2: Total number of occupational diseases reported through annual medical reports per region for 2021 and 2022 (DMRE, 2023)

The current practice of establishing OELs to reduce exposure to RCS is to relate the dose response to the weight of RCS, and the OELs are expressed in mass per volume (mg/m^3). If the personal exposure is above the OEL, there is a formal investigation. Currently, such an investigation focuses on the mass of RCS, the reasons for the over-exposure and changes to the controls (DMR, 2018) but not on the particle size of RCS.

Other factors may contribute to the toxicity of RCS, such as the polymorph present (quartz, cristobalite, and/or tridymite), the particle size, surface reactivity, reactive oxygen species on the surface of silica, the age of the mechanically fractured RCS, and the mineralogical composition of the RCS-containing dust (OSHA, 2013).

1.3 Problem Statement

The routine practice to determine personal exposure to RCS is to measure the RCS mass in a sample of airborne dust that has been captured in the breathing zone of the employee. The sample of dust is captured using a cyclone (i.e. size selective sampler) that has a median cut size of approximately 4 µm. The mass of respirable particles typically consists of particles less than ten micron. However, depending on the source and nature of the dust, a substantial number of particles less than one micron in size may be present.

The personal exposure sample represents the respirable fraction of the airborne workplace dust that less than ten micron according to the ISO definition (ISO, 1995). Figure 1.3 shows the different particle size fractions that are of concern for workplace exposures to airborne pollutants. The finer the particle size of dust, the deeper it can go into the airways of the human and the more difficult it becomes for the body to remove the dust.

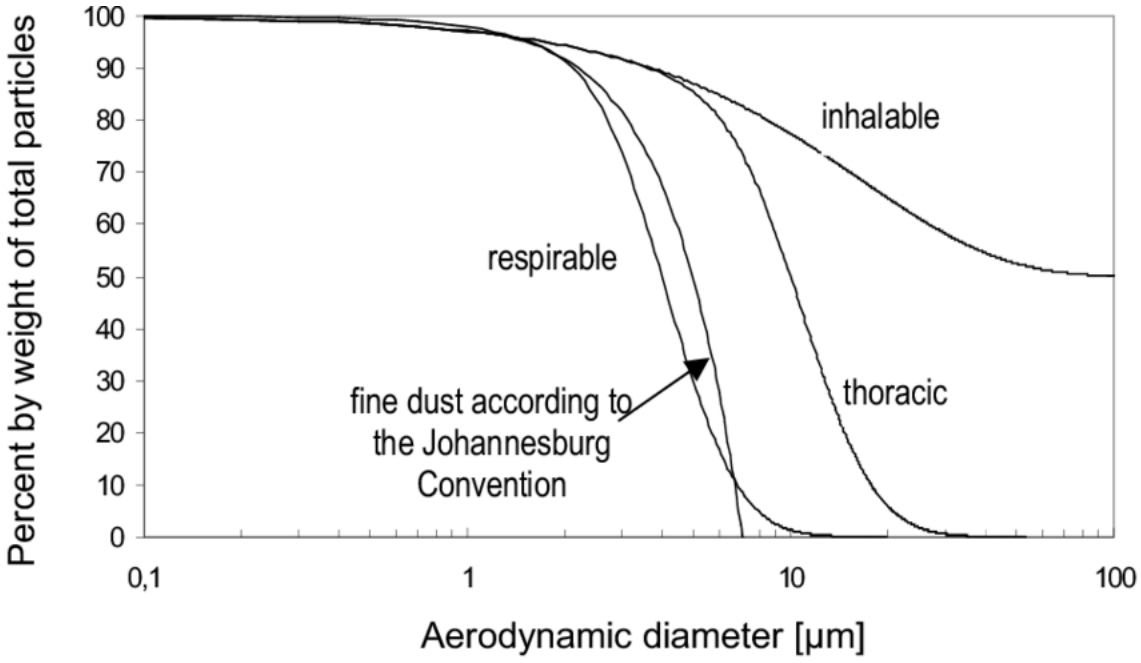

Figure 1.3: Inhalable, thoracic, and respirable conventions and fine dust fraction according to the Johannesburg Convention. (Hebisch et al., 2005)

Following the sampling, the crystalline silica content is determined by laboratory analysis. However, the resulting PSD of RCS particles contained in the captured dust has not been comprehensively characterised and there is still information lacking (Chubb & Cauda, 2017). It is assumed that RCS has the same PSD as the non-RCS dust in a respirable sample. Hall et al. (2022) related the RCS concentration in the different size fractions of dust but did not measure the RCS particle size. Although the OEL is relevant to the respirable fraction of dust, the actual particle size of RCS is not factored in when the OEL is established. The characterisation of the particle size of RCS in dust is still lacking.

1.4 Justification for the Research

The elimination of silicosis is a global and national priority in occupational health, especially in workplaces where workers are exposed to airborne dusts that contain RCS, such as ore drilling and crushing, milling, or packing of RCS-containing products. The DoEL and

Department of Mineral Resources and Energy (DMRE), together with industry and organised labour, are committed to holding industry accountable and protecting employees from workplace exposure to RCS. Since the implementation of the National Programme for the Elimination of Silicosis (NPES) in 2005 (DOL, 2005), and despite the commitment of all stakeholders to the programme, silicosis has not been eradicated, even though exposure of workers to the mass concentration of RCS has been reduced. It is possible that other aspects of RCS, such as particle size, may be implicated in the toxicity of RCS (Pollard, 2016; Keles et al., 2022). The PSD of RCS is one aspect that must be understood to eliminate silicosis effectively (NIOSH, 2002). The PSD of RCS has not sufficiently been explored and this study investigated the measurement of the particle size of RCS in archived dust samples.

1.5 Research Question

The DMRE implemented an OEL for RCS of 0.1 mg/m^3 in 2006 (DME, 2006). The mining industry has made significant progress by reducing worker exposure to below this OEL, but despite all efforts, silicosis is still prevalent. Adopting the hypothesis that PSD_{RCS} may be a relevant characteristic for the toxicology of RCS, this study addresses the research question: Can the PSD of total respirable dust, when routinely measured by the laser light scattering (LLS) method, give an accurate PSD of RCS as measured by using the scanning electron microscopy (SEM) method (the gold standard for PSD)?

1.6 Study Aim

The aim of the study is to determine whether the PSD measurement of all dust particles (RCS and non-RCS particles), using the LLS method ($PSD_{LLS(Dust)}$), represents the particle size measurement of the respirable crystalline silica contained in the dust sample, as measured by the SEM method ($PSD_{SEM(RCS)}$). The LLS method is faster and more affordable than the SEM

method. By measuring the PSD of all the dust particles in the respirable dust sample using LLS and comparing it with the PSD of RCS particles using SEM, it may be possible to show that the distribution obtained by LLS represents the PSD of RCS.

1.7 Study Objectives

The study has three objectives:

Objective 1: To operationalise the Scanning Electron Microscopy (SEM) method for accuracy and effort in measuring the particle size in respirable dust samples of NIST, Arizona, and gold mine dust, through the selection, the number of individual particles to be analysed and the accurate sizing of these particles.

Objective 2: To compare the particle size distribution (PSD) attained by the Laser Light Scattering (LLS) method with the particle size distribution achieved by the Scanning Electron Microscopy (SEM) method, in order to show the relationship between the results obtained by the two methods, in NIST, Arizona, and gold mine dust.

Objective 3: To estimate the particle size of respirable crystalline silica (RCS) from $PSD_{LLS(Dust)}$ and compare the estimated RCS particle size results with measured RCS particle size data ($PSD_{SEM(RCS)}$) in NIST, Arizona, and gold mine dust.

The following sections of the report outline the approach that was followed to address the aim and the objectives of this study.

Chapter 2: Literature Review

2.1 Introduction

The literature review provides a background on silicosis and the significance of the particle size distribution of RCS. The different particle size measurement methods are discussed.

2.2 Background on Silicosis and Respirable Crystalline Silica

The current consensus is that the health outcomes associated with exposure to free RCS particles are affected by the mass concentration of the RCS, i.e. RCS weight per volume of air. Although the concentrations of RCS-containing dust that employees are exposed to have been significantly reduced since the implementation of the national elimination programme, silicosis has not been eradicated (Knight et al., 2015). Nearly 200 cases of silicosis per 1 000 mine employees are still being reported per annum in South Africa (NIOH, 2021). Even globally, silicosis has not been eradicated as an estimated 65 000 deaths related to silicosis were still reported as recently as 2019 (ILO, 2021)

The exact properties of RCS that are responsible for the development of silicosis have not been clearly defined (NIOSH, 2002; Pollard, 2016).

Fubini et al. (2004) have shown that the reactive oxygen species on the surface of RCS particles may be related to the toxicity of RCS. Pavan and Fubini (2017) found that a combination of reactive groups on the surface of the RCS particles triggers an inflammatory response, leading to a sequence of events as the body tries to remove RCS. The inability of the body to effectively remove RCS, and the continued presence of RCS, ultimately leads to the onset of disease (Pollard, 2016).

There was debate about the role of the RCS polymorph and its associated toxicity. However, in a 2001 study, observed trends in the exposure-response between cristobalite and quartz did not differ significantly (Steenland et al., 2001). OSHA concluded that the toxicity of RCS does not differ between the different polymorphs of RCS. Accordingly, the OSHA-revised permissible exposure limit for RCS applies to all the polymorphs (OSHA, 2016).

A relationship between the toxicity of RCS and the age of the fractured (i.e. mechanically broken) particles has been established. A positive correlation has been found between the development of acute silicosis and RCS-containing dust that has been newly milled or crushed (Castranova, 2004).

The natural coating of RCS particles with other mineral compounds may increase or decrease the toxicity of RCS. The associated inflammatory response may also influence the onset of silicosis (Wallace et al., 1996). Some of the dusts that may coat the RCS particles and reduce the toxicity of RCS are aluminium salts, polyvinylpyridine-N-oxide polymer, and organosilanes (Pavan and Fubini, 2017).

Although there is a relationship between the PSD of dust and the RCS concentration found in the dust of a similar PSD (Qi et al., 2016), the PSD of RCS (PSD_{RCS}) contained in the dust has not been characterised and requires further research (Chubb & Cauda, 2017). Hall et al. (2022) characterised the PSD of dust emissions from cutting and grinding artificial stone, that is made up of resin and mineral dusts. The RCS concentrations were similar in the different size fractions that were sampled. The PSD of RCS was not characterised in this study.

2.3 Significance of Particle Size

The focus of this study was on the PSD of RCS in the respirable dust of archived dust samples. The importance of PSD is that particles that are in the size range of < 10 µm can enter the

deepest areas of the lung and be deposited in the gas-exchange regions (WHO, 1999). On deposition, the particles, which represent a large surface area of crystalline silica, interact with human tissue. This interaction leads to the onset of disease: RCS particles cause damage to lung tissue, and during the body’s attempts to repair the damage, scars are formed. These scars or fibrosis are called silicotic nodules, and these nodules are the diagnostic characteristic of silicosis (Rees & Murray, 2007).

While small particles remain suspended in the air for longer periods owing to the aerodynamic nature of the particles, in terms of occupational exposure the interest is in the aerodynamic particle size diameter (APSD). APSD is important as it refers to "the diameter of a hypothetical sphere of density 1 g/cm^3 having the same terminal settling velocity in calm air as the particle in question, regardless of its geometric size, shape and true density” (ISO, 2016). APSD describes the ability of the particle to enter, distribute, and deposit in the respiratory tract of the body (e.g. nose, mouth, lungs).

The particle size of approximately 2 µm has a greater than 70% probability of depositing in the gas-exchange region of the lungs (ISO, 1995). Larger particles more effectively deposit in the higher airways and are subsequently removed through the normal protective functions of the body (WHO, 1999).

In order to determine an employee’s personal exposure to harmful pollutants, a sample is taken from the airborne dust available for inhalation. Samples are taken using a sampling train that consists of a sampling pump linked via tubing to a cassette. The cassette contains a membrane filter that is pre- and post-weighed to determine the mass of the dust collected. Connected to the cassette is a cyclone (i.e. size-selective sampler) that should ensure that only airborne dust within the respirable size fraction is sampled and deposited onto the filter. Further elemental

analysis is conducted to identify the concentration of the harmful pollutant of interest, in this case RCS.

When taking samples in the workplace, it is very important that a respirable dust sample is representative of the employee’s personal exposure during the sampled shift. The mass and the PSD of the dust that is collected and deposited on the filter depend on the performance of the sampling pump and the cyclone.

A sampling pump’s pulsation can vary by more than 10% over a sampling period and is dependent on the pump model (Lee et al., 2014). When a cyclone is fitted, the pulsation can vary by up to 25% over a sampling period before the sampling efficiency is affected and personal exposure is underestimated (Lee et al., 2014). Sampling pumps are required to comply with ISO 13137 (ISO, 2022) to ensure that they maintain the calibrated flow rate and pulsation throughout the sampling period.

Cyclones are designed to comply with the ISO/CEN definition as described in ISO 7708 (ISO, 1995) so that only airborne dust from the respirable fraction is sampled. The particle size selection of samplers affects the mass concentration of the resulting samples as well as the measured RCS concentration (Stacey et al., 2013, Page, 2006, Stacey et al., 2013, Mecchia et al., 2013). In previous studies, the PSD of the dust that was captured and deposited on membrane filters by South African samplers was measured using Laser Light Scattering (LLS) (Pretorius, 2011a; Pretorius, 2011b). In these studies, the median diameter of the dust, as determined by Laser Light Scattering, was approximately 3 to 4.9 µm. These studies focused on the particle size of the dust deposited on the filters and the subsequent impact on the determination of the RCS concentration. These studies did not examine the particle size of RCS specifically, but only considered the particle size of all dust particles.

PSD is also important when further elemental analysis is conducted to quantify the mass concentration of RCS. Two analytical techniques are used to measure the concentration of RCS: X-ray Diffraction (XRD) and Fourier-Transform Infrared (FTIR). Both techniques are sensitive to the PSD of the RCS measured (Page, 2006, Mecchia et al., 2013). The XRD response, and thus the subsequent RCS mass concentration that is derived, can vary as a result of the sampler performance (Mecchia et al., 2013, Pretorius, 2011b).

Unfortunately, there are no South African standards with which sampling pumps and cyclones must comply. For now, it is assumed that the manufacturers’ quality control ensures that samplers and pumps that are produced provide, at the very least, consistent performance.

2.4 Laser Light Scattering (LLS)

Different analysis techniques are employed for determining the size distribution of deposited particles. These techniques include particle counting, gravimetric sedimentation, light scattering, and particle measurement. Only two particle size analysis techniques are discussed in this study: LLS and SEM.

LLS is a technique whereby particulates in a suspension are subjected to a laser beam and the particles scatter the light based on their size as shown in Figure 2.. Two light sources are used, namely, 650 nm red laser diode (1 in the figure below) and a 405 nm blue laser diode (LED) (2 in the figure). The scattered light is captured on detectors or photodiodes (3 and 4) and the particle size distribution is mathematically derived using the Mie Theory based on the different angles at which the light is scattered. The light scattering is detected in 93 channels (1 nm to 3 mm) and the algorithm assumes that the particles are spherical.

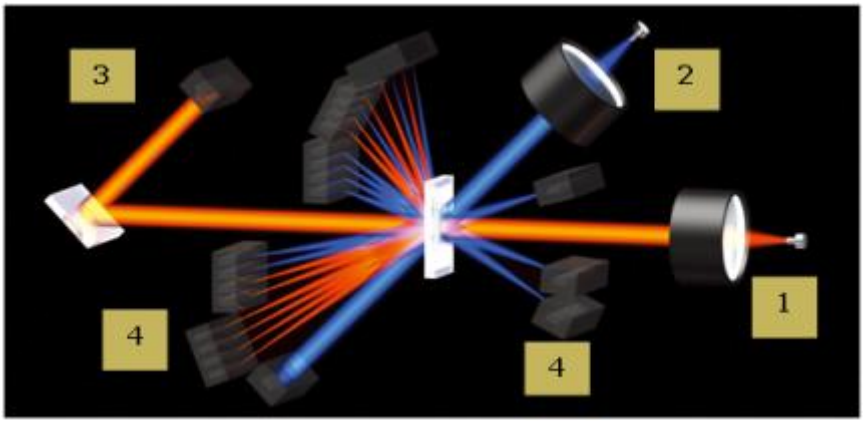

Figure 2.1: Illustration of laser light scattering (Horiba, 2007)

The Mie Theory was developed by Gustav Mie as an optical model to calculate the size distribution of particles (Garbin et al., 2009, Horiba, 2007). This technique uses the refractive index of light for a compound (e.g. mineral dust) in a suspension medium (e.g. water) (ASTM, 2014). According to ISO 13320:2020 the Mie Theory is applicable for analysis over a dynamic range of 0.1 µm to 3 mm (ISO, 2020). For sizes outside this range, other models will have to be applied such as the Fraunhofer Theory (Horiba, 2007).

The LLS technique was used to measure the PSD of all dust particulates in a sample ($PSD_{LLS(Dust)}$), i.e. the PSD of RCS and non-RCS particulates.

Certain aspects were considered for the LLS method for this study, namely:

a) Effective removal of the dust from the filter

In order to conduct the measurement on the LLS instrument, the airborne dust that was deposited on the filter membrane should be removed and suspended in a liquid medium (e.g. water or iso-propanol). Removal of the dust is done by placing the filter with dust in a liquid medium and then loosening the dust through vibration using an ultrasonic bath (ASTM, 2014).

Effective removal of all the dust is important to ensure the measured PSD is representative of the entire sample. The laboratory SOP addressed this aspect during the method validation process prior to accreditation (ISO, 2017).

b) Sample concentration

During the PSD measurement, the instrument indicates the transmittance of the laser light through the sample. The transmittance is affected by the sample concentration, which is not necessarily a mass concentration but a particle density concentration. For optimal results, the transmittance must be within the range 75% to 90% pass-through in order for the PSD to be calculated (Horiba, 2007). If the sample concentration is too low, the transmittance goes above 90%, there are not enough particles to diffract the laser light. If the transmittance goes below 75%, there are too many particles, and the system cannot distinguish between individual particles. However, high-concentration samples can be diluted with the liquid medium to improve the transmittance.

Based on the guidance from the instrument supplier and the researcher’s experience with LLS analysis, the concentration should be sufficient for the analysis if the researcher can see the colour of the airborne dust on the filter (i.e. the discolouration is visible).

c) Refractive index used

The LLS method requires the use of the refractive index of the sample that is measured. Airborne dust from gold mines consists of a combination of minerals, each having their own refractive index (Horiba, 2007). However, the values are in the same range as that for RCS, namely 1.54. A refractive index of 1.54 is used initially and the value is numerically adjusted on the software until there is agreement between the theoretical and actual measurements; i.e.

the chi^2 value is less than 1.0. This agreement should be verified for each sample to ensure that the optimal refractive index value is used during measurements (Horiba, 2007).

2.5 Scanning Electron Microscopy (SEM)

SEM analysis is a technique which uses the wave properties of electrons to make greatly magnified images of objects. The electron ‘gun’ of the SEM accelerates electrons to high energy. These highly accelerated electrons are fired at a sample and three different signals are given off: backscattered electrons, secondary electrons, and Energy Dispersive X-rays (EDX). Backscattered electrons are a result of electrons bouncing back from the sample, known as elastic collision. The EDX (also known as EDS) are used to determine the elemental composition of a sample, i.e., silicon, aluminium, iron. The secondary electrons are created when the electrons from the SEM source loosen electrons from within the sample, known as inelastic collisions. Figure 2. illustrates how the incident electron beam emits different signals.

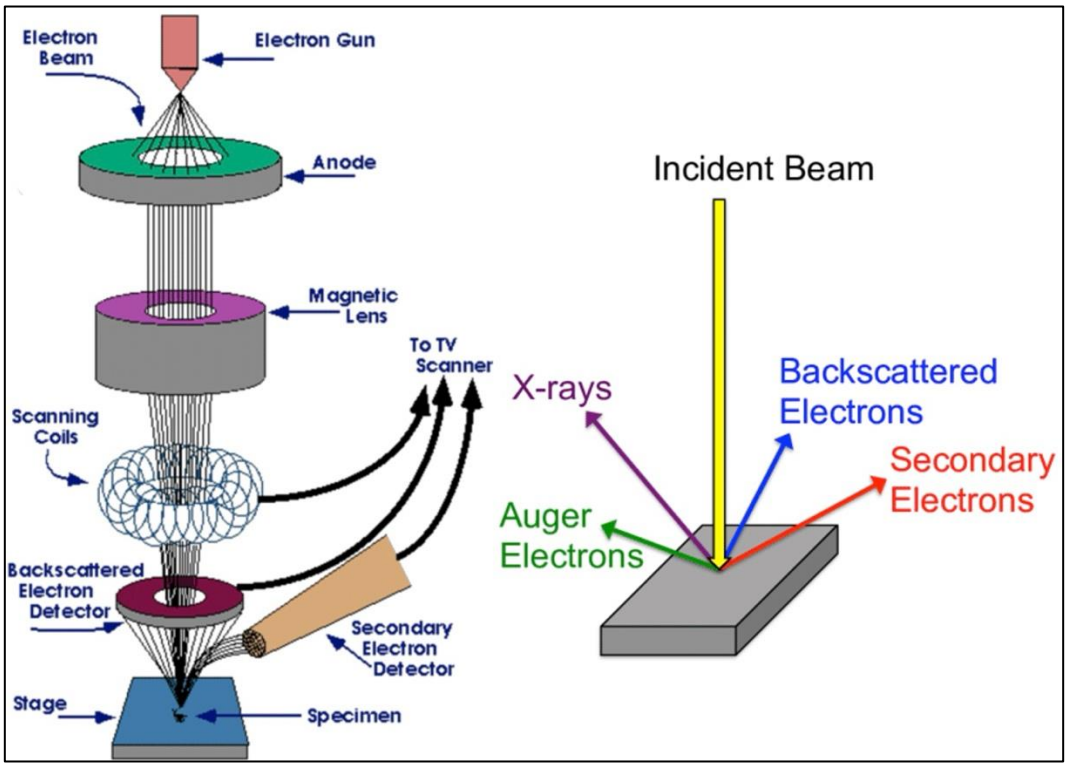

Figure 2.2: Diagram to illustrate SEM (Walock, 2012)

Detectors detect the different signals that are emitted as a result of the interaction between the fired electrons and the sample, and a magnified image is created.

The United States Environmental Protection Agency (US EPA) developed a method for the measurement of dust particles using SEM-EDS (EPA, 2002). The method was designed to measure the size, composition, and morphology of ambient particulates in an attempt to identify the sources of pollution. The method depends on the particulates being caught on a filter medium with the following characteristics:

- It has a smooth and flat surface and does not allow particles to penetrate beyond the surface.
- It is transparent to x-rays in the EDS spectrum
- It can withstand heat from the electron beam
- It is electrically conductive to dissipate an electric charge from the sample
- It is blank and with minimal impurities that will affect the EDS spectra
- It is sturdy and durable to withstand handling (EPA, 2002).

Typically, polycarbonate filters are used due to the low background signal obtained in SEM analysis. Mixed cellulose ester (MCE) filter membranes were found to allow better capturing and adhesion of micro- and nanoparticles (Diez-Gil, C et al., 2008). However, MCE filters can have a ‘noisy’ background which may interfere with the SEM analysis, but when treated with a solvent, the MCE material has a more uniform surface and reduced background noise (Getman et al., 2017).

The sizes of selected particles can be determined by image acquisition and processing software. EDS enables the selection of particles with a specific composition for inclusion in the image analysis, such as silica particles.

Sellaro et al. (2015) developed a manual method to measure a total of 500 dust particles on three respirable dust samples. Using this method, these authors found that, depending on where the samples were taken in the workplace, the elemental composition of the measured particles might differ significantly. This method can be quite time-consuming, however, and in itself is not practical for implementation as a routine method. Johann-Essex et al. (2017) went further to develop a computer-controlled SEM-EDS (CCSEM-EDS) method for the routine measurement of coal mine dust particles, an alternative method to use for routine application. The computer-controlled method enabled the measurement of 500 dust particles less than ten micron in diameter. The aim was to determine the size, shape and elemental composition of the dust particles in different mine samples, and not the RCS particles specifically.

Sarver et al. (2021) went further to characterise the particle mass and number fractions in mine dust using SEM-EDS. The data was classified according to different mineral classes, including silica, where the RCS particle mass % distribution in the dust samples across 25 mines was found to be between 50% and 80%. The particle size of silica was found to be greater than 400 nm, a very interesting finding following the application of SEM-EDS.

SEM-EDS is useful in characterising the size and mineral composition of particles. Keles et al (2022) applied SEM-EDS to respirable coal dust from mines and found silica to be finer than the other particles. Furthermore, during analysis the authors found that silica particles were at times covered by or agglomerated with other mineral particles.

Accordingly, there was a need to determine the RCS particle size among non-RCS particles in South African gold mine dust. Certain aspects were considered for the SEM method for use in this study, namely:

a) Type of dust

Gold mine dust consists of minerals that are plates or sheet-like. Since SEM is a surface technique, a potential challenge may be to identify RCS particles that are fully or partially covered by these plate-like minerals (Keles et al., 2022).

b) Particle density

This method will require that particles be easily distinguishable from one another. A high particle density in the area of measurement may complicate the analysis i.e. result in under-reporting of the particle size (Keles et al., 2022). Particle density in one specific area on the sample is not directly related to mass concentration, and initial particle size measurements will indicate if there is an upper mass concentration limit i.e., the dust load is too high for accurate particle size measurements.

c) Uniformity of deposition

A specimen will be taken from the centre of the filter membrane and for this reason the uniformity of dust deposition is important. Previous studies that involved South African-made cyclones indicate that the dust deposition is sufficiently uniform for this study (Stacey et al., 2013).

2.6 Comparison between the LLS and SEM methods

Table 2.1 provides a comparison between the SEM and LLS methods in terms of operational aspects.

Table 2.1: Comparison between the SEM and LLS methods for PSD measurements of RCS and all dust particles including RCS

Specification	**SEM**	**LLS**
High-level comparison	Labour-intensive and time consuming	High throughput method
Specimen size	Specimen taken from the membrane filter	All the deposited dust particles once removed from the membrane filter
What is measured?	PSD of particles with a specific mineral composition such as RCS, aluminium-silicates	PSD of all the respirable dust particles in the sample
Information obtained	Specific information about an RCS particle (e.g. size, shape, elemental composition, visual image and particle density. Aggregation of size of analysed particles will provide PSD	PSD of total dust particles in the sample (i.e. total dust distribution) in the range of 1 – 10 µm (respirable dust)
Unit of measure	Length (L), width (W), spherical diameter (ds), cross-sectional diameter (dc) and volume (Vol) of approx. 200 RCS particles. Median PSD in micron (µm) is reported	PSD expressed as volume (Vol), number (Nr), length (L) and area, in micron. Median PSD in micron (µm) is reported
Approximate instrument cost	Above R 2 million	R 500 000 to R 1 million
Operational costs	Annual maintenance and service costs; liquid nitrogen (± R 30 000 – R 60 000)	Annual maintenance and service costs (± R 30 000)
HR skills required	Sophisticated analysis; requires high level of skill	Relatively simple application; requires lower level of skill
Sample preparation	30 to 60 min	5 to 10 min
Analysis time	3 to 4 hours	3 to 5 min

Although LLS is affordable, simple to use, and can be conducted within a short time period, it is clear that the biggest advantage of SEM is the vast amount of information that can be obtained from individual particles (Hegel et al., 2014). The application of both techniques on the same sample provides additional information when evaluating the morphology of particles

(Grubbs et al., 2021). For this reason, this study aims to determine whether $PSD_{LLS(Dust)}$ can provide relevant information about the particle size of RCS in respirable dust samples consisting of a mixture of RCS and non-RCS particles.

Chapter 3: Methods

3.1 Introduction

This chapter presents the methodology of the study and covers the study design, study site, population, data-collection and analysis methods. In this chapter, the sample preparation and particle size distribution (PSD) analysis are explained for the SEM and LLS analytical methods. The chapter then describes the methodology used to compare the PSD data results obtained from the two analytical methods to address the objectives of the study.

3.2 Study Design

This observational study aimed to determine the PSD of archived respirable dust samples by laboratory analysis to investigate the particle size of RCS in dust samples. Figure 3. provides an overview of the flow of the study.

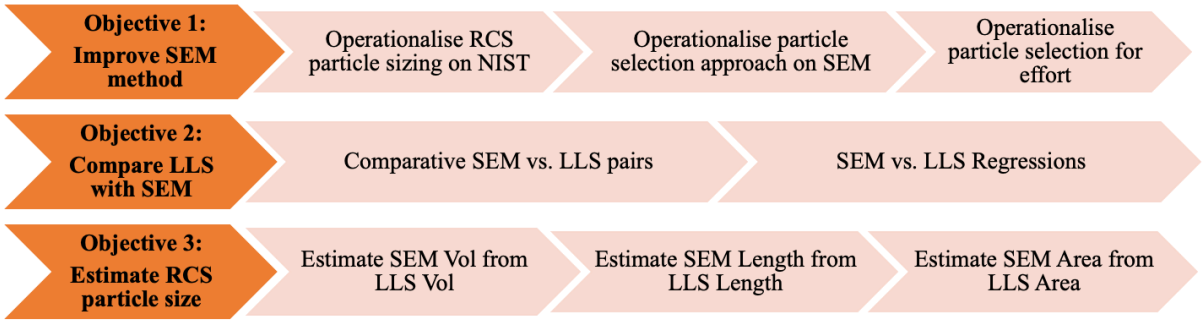

Figure 3.1: Flow of the study for achieving the results in line with the study objectives

3.3 Study Site

The study was carried out in Pretoria in Gauteng Province, South Africa, in two analytical laboratories: the laboratory of the National Metrology Institute of South Africa (NMISA) and the Air and Dust (A&D) Laboratory of the Council for Scientific and Industrial Research (CSIR).

NMISA was established under the South African Measurement Units and Measurement Standards Act, No. 18 of 2006 (The Measurement Act). NMISA participates in the International Metre Convention (which dates back to 1875) and its organs, the International Committee for Weights and Measures (CIPM) and the Convention of the International Bureau of Weights and Measures (BIPM). NMISA’s analyses and measurements are traceable to the International System of Units (NMISA, 2022).

The CSIR’s A&D Laboratory is accredited to the South African National Standard (SANS) 17025 in the South African National Accreditation System (SANAS). The particle size analysis method using LLS (i.e. ASTM C1070) is shown on the A&D Laboratory’s schedule of accreditation (SANAS, 2020).

3.4 Study Population

The population that was available for study was more than 200 archived respirable dust samples that had been sent to the A&D Laboratory for RCS analysis and subsequently archived.

The respirable dust samples contained different mineral matrices and had been prepared for different purposes:

a) Approximately 30 samples were prepared from the standard reference material (SRM) of alpha-quartz (i.e. pure silica (SiO_2)) from the National Institute for Standards and Technology (NIST) (NIST, 1999). These samples were prepared in the laboratory in 2012 as calibration standards to measure silica on XRD. A known mass of the NIST dust was deposited onto 25 mm diameter membrane filters (MCE and silver) in a dust chamber using a size-selective sampler with a cut-point of 4 μm, i.e., the sampler collects particles with a size of 4 μm with 50% efficiency. After the XRD instrument response was calibrated against a known mass of NIST, the samples were archived.

The material safety data sheet (MSDS) of NIST showed the PSD that was measured using LLS. It is acknowledged that the instrument settings and analysis conditions were not interrogated and compared with those used in this study.

b) Approximately 30 samples were prepared from the standard test dust ISO 12301-1, also known as Arizona Ultrafine Dust. This dust consists of pure silica mixed with other known minerals and the composition is provided on the material safety data sheet (MSDS) (Powder Technology, 2008). These samples were prepared in the laboratory for a research project undertaken during the period 2010 to 2011 (Pretorius, 2011b). A known amount of Arizona dust was deposited onto a 25 mm diameter MCE membrane filter in a dust chamber using a size-selective sampler with a cut-point of 4 μm. After the research project was concluded, the samples were archived.

c) The remainder of the samples were taken in a South African gold mine as part of its occupational measurement programme in 2012 to monitor employee exposure to RCS in the workplace. The personal exposure dust samples were taken using a size-selective sampler with a cut-point of 4 μm and the respirable dust was deposited on 25 mm diameter MCE filters. The samples were numbered and sent to the CSIR A&D Laboratory for the mandatory measurement of silica using non-destructive XRD analysis (MDHS 101/2, n.d.). After analysis, the samples were archived.

3.5 Study Sample Size

There is no prescribed sample size to use when comparing two analytical methods, such as for the measurement of the sample PSD using LLS and SEM. Different analytical methods have different conventions regarding sample size, but with these two methods there is no known convention. As part of the methodology adopted for Objective 1, however, the number of particles to measure with SEM was operationalised for accuracy and effort to measure within

repeatable measures. Sellaro et al.’s (2015) method was used as guidance where 100 particles were measured on each of three samples. Consideration was given to the total number of samples that could realistically be measured during the time available for this study. SEM analysis requires one day per sample and 80 days were made available for 80 samples at a maximum. However, the final number of samples to be analysed depended on the outcome of Objective 1 after the SEM method was improved for accurate measurement of RCS particles. Originally, 25 samples were targeted for both LLS and SEM analysis.

3.6 Data-collection Methods

The data i.e. the particle size distribution (PSD) of the RCS particles on the filter, were collected using the SEM and LLS methods as described in the sections below. It should be noted that for SEM analysis the actual size of individual particles of a sample is measured, and the cumulative PSD used throughout the report is the cumulative probability distribution of the sample over a size range (refer to Section 3.10.1.). In contrast, LLS only reports the cumulative probability distribution of the sample and not the sizes of individual particles.

Section 3.6.1 describes the detailed sample preparation for the SEM method and the preparation of the instrument for analysis. How the PSD data were obtained from SEM is explained in terms of how particles were measured and selected.

Section 3.6.2 describes how the PSD data were obtained from the LLS method.

3.6.1 Scanning Electron Microscopy (SEM) Analysis to Determine $PSD_{SEM(RCS)}$

3.6.1.1 SEM Sample Preparation

The sample preparation for the SEM method followed generally accepted methodologies (Sellaro et al., 2015; EPA, 2002). The archived respirable dust samples were generated by sampling airborne dust with a pump–cyclone combination where the respirable fraction was

deposited onto a 25 mm filter membrane. Figure 3.2 shows a typical sample that is used for the measurements. The filter media of the archived dust samples were either MCE or silver filters. It is acknowledged that ultrafine particles may be embedded in the filter membrane, at a depth that depends on the nature of the filter membranes, and may not be visible by the surface analysis of the SEM.

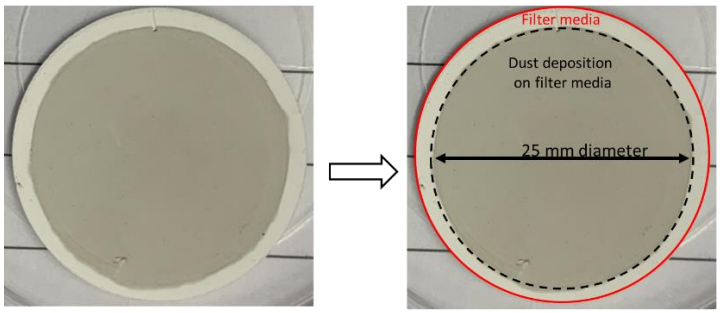

Figure 3.2: A typical sample of respirable dust

Assuming uniform dust distribution, one 1.13 cm^2 specimen (i.e. a stub to fit onto the SEM sample holder) was removed from the centre of the respirable dust sample using a punch. The punch, shown in Figure 3.3, proved to be effective in cutting a circular specimen (hereafter referred to as the “stub”) without causing damage to the rest of the filter, which was preserved for use in the LLS analysis.

Figure 3.3: Punch that was used to remove a specimen from the sample

Figure 3.4 below shows a typical sample before and after the stub was removed from the sample, using the punch.

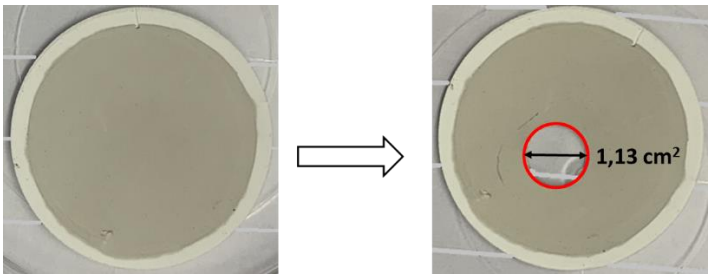

Figure 3.4: Typical sample before and after removal of the stub

The stub was secured with double-sided tape onto a disc and could not be removed after analysis. The disc was placed on a 14-position sample stage (Figure 4).

Figure 4: Stub secured to disc that is placed on sample stage

To make the dust on the stub more conductive during SEM analysis, the stub was coated with carbon. An EMITECH K950X carbon evaporator (shown in Figure 5) was cleaned with a moist lint-free cloth prior to use and the sample stage that contained the stubs on the discs was placed inside the evaporator.

Figure 5: Stubs on sample stage placed inside the carbon evaporator

Two graphite rods were connected to the inside of the evaporator lid (Figure 6). These rods were spring-loaded to put them under pressure so that they made contact at their tips.

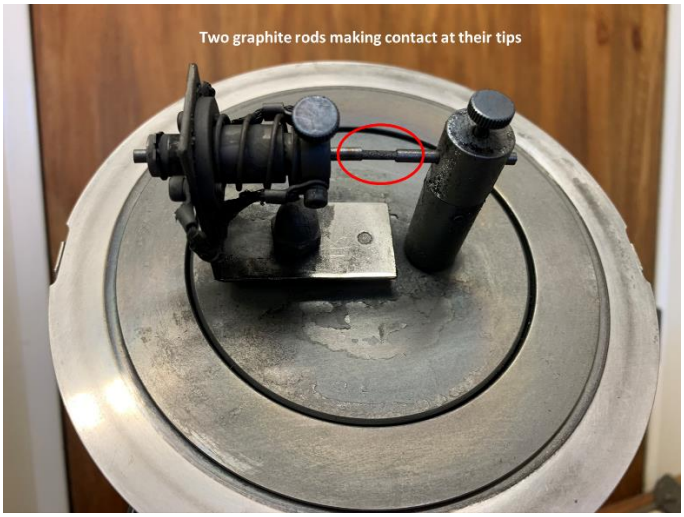

Figure 6: Two graphite rods made contact at their tips

The evaporator was closed, and a vacuum was created inside for approximately five minutes. The rods were heated and, when they melted at the contact-point, carbon fumes were formed that settled on the stub and coated the dust with a thin layer of carbon. Figure 7 shows the closed evaporator when the dust samples were coated with carbon. During the outgassing

process, the rods glow red-hot for a few seconds. The process of heating the rods was carried out twice. The sample stage was rotated to ensure uniform coating of the dust samples.

Figure 7: Coating of samples using carbon evaporation

On completion of the carbon coating, the evaporator was stopped and vented. The evaporator was opened after venting and the sample stage was removed.

3.6.1.2 SEM Method Preparation

The SEM instrument was prepared according to its specified NMISA Standard Operating Procedure (SOP). The sample stage was removed from the evaporator and was placed inside the SEM instrument (Figure 8), which was a Zeiss Crossbeam 540 containing a Gemini 2 column with an X-Max Extreme Energy Dispersive Spectroscopy (EDS). Various detectors were connected to the instrument to capture the different electrons being emitted. The detector used for this study was the backscatter electron detector which provided atomic number contrast imaging.

Figure 8: SEM instrument

The SEM instrument was first vented to obtain a vacuum of between -5 and -9 mbar. The electron ‘gun’, which generates and ‘shoots’ the electron beam, was under -9 mbar of pressure.

An area was selected on the stub and, using 500× magnification, a visual image of an area of 228 x 159 µm was seen. The analysed area is shown in Figure 9, where the white spots represent dust particles.

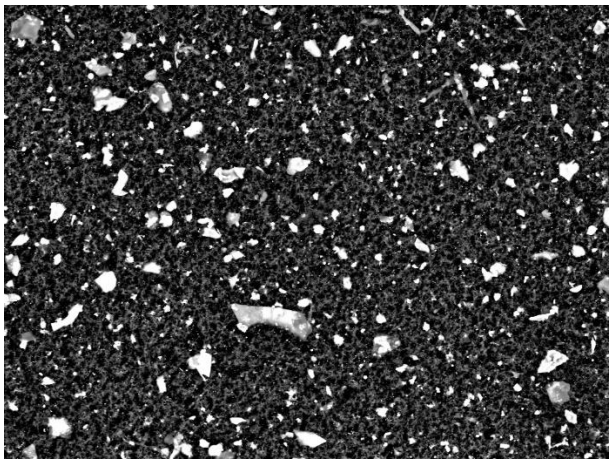

Figure 9: Visual image of an area on the stub

The EDS detector measured the X-rays that were emitted when the sample was bombarded with the highly accelerated electrons. Each element on the periodic table emits X-rays at specific electron volts (eV), which makes it possible to identify an element. Silicon (Si) emits X-rays at 1.74 kilo electron volts (keV). Figure 10 shows an example of an EDS spectrum for the entire field of view of a gold mine dust sample that contains mostly aluminium (Al), with traces of other elements such as silicon, iron, sodium, potassium and magnesium.

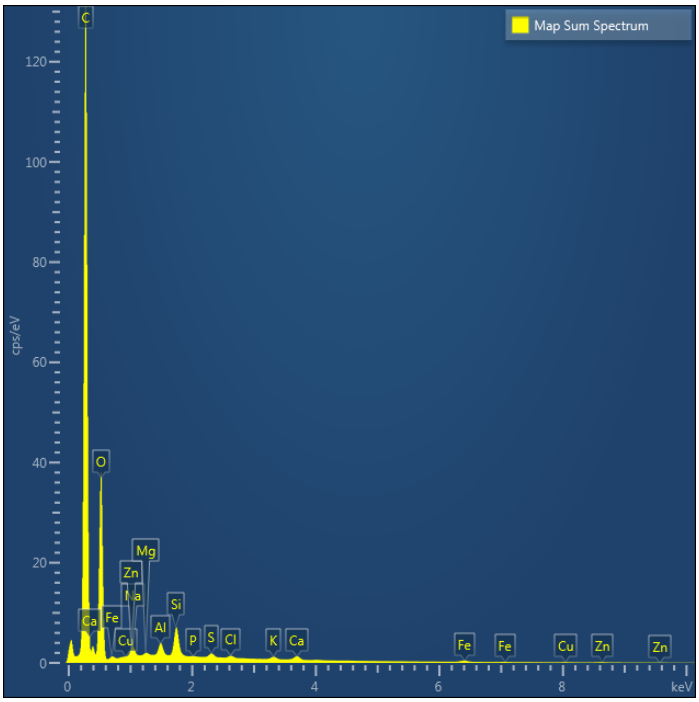

Figure 10: EDS shows the elemental composition of each particle on the sample

X-ray mapping uses the data obtained from the EDS detector to distinguish the silica particles – that is, the particles with a elemental composition of SiO_2 – from the other particles that have a different composition. Figure 11 shows how X-ray mapping was used to distinguish particles with different elemental compositions from one another.

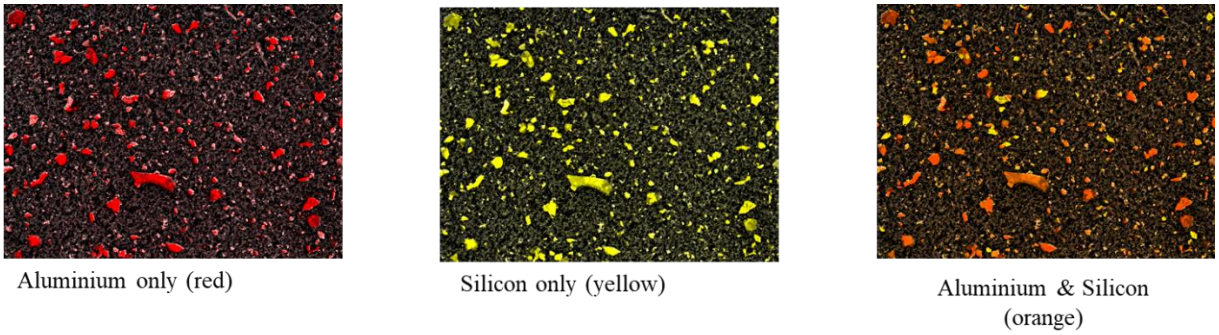

Figure 11: X-ray mapping of some elemental compositions

The image on the right illustrates that when both aluminium and silicon are mapped, they are shown as orange, with the remaining silica particles shown in yellow.

The phases of the yellow particles were analysed with EDS to confirm that their elemental composition was silica, i.e. SiO_2 (Figure 12). The sample matrices used in this study consisted mostly of crystalline material (silica and non-silica). The focus of this study is on the size of silica particles only. It is acknowledged that EDS does not provide a measure of crystallinity. When EDS confirms the composition of a particle as silica, it was assumed that it is a crystalline silica particle. Given that the sizes of the silica particles are within the respirable range, reference to respirable crystalline silica (RCS) will be made hereafter.

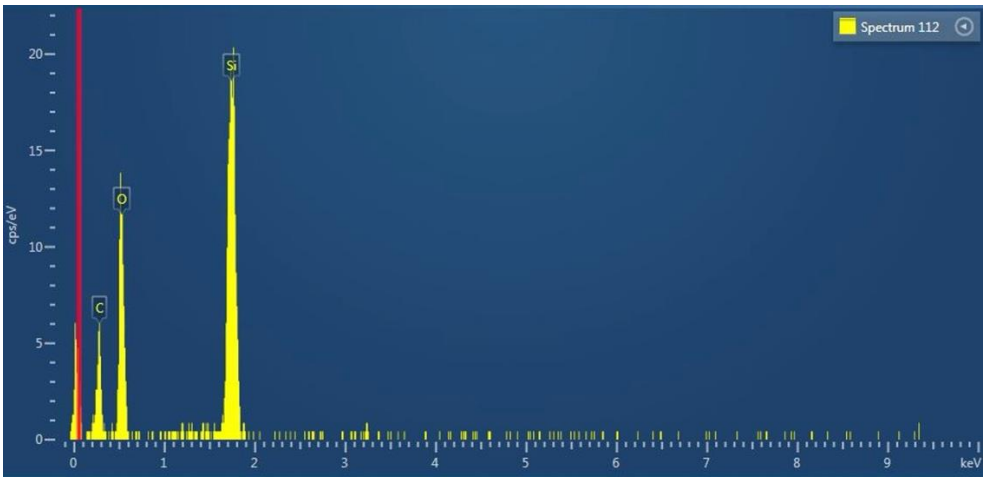

Figure 12: EDS confirms the presence of SiO_2 dust with the carbon coating to improve conductivity

The X-ray mapping was found to be an effective way to identify and select silica particles for PSD measurement. It took approximately 20 minutes to identify 20 particles.

Five areas were selected on each stub and 20 silica particles were manually selected in each area from the visual image, so that there was a total number of 100 particles per archived dust sample. (It is acknowledged that this approach has an inherent user bias. The researcher deliberately selected a range of small, medium and large particles to avoid only selecting larger, brighter particles.)

3.6.1.3 Determination of particle size using SEM

The visual image obtained from the SEM method was imported into the ImageJ software (NIH, 2018), which was the software selected for analysing the sizes and diameters of the particles. ImageJ software was originally developed by the National Institute of Health (NIH) in the USA and is used to gather and process data from scientific images (NIH, 2018). ImageJ is open-source software and over the past 25 years, scientists from different disciplines collaborated on improvements to make ImageJ the preferred software for image analysis.

The line tool of this software was calibrated by measuring the legend on the SEM image (i.e. 50 µm). The scale in the software was set at 50 µm, and the units of the particle dimensions were measured in micron (µm).

The ImageJ software can auto-analyse all the dust particles; however, within the scope of this study, the focus was on the size of RCS particles only (i.e. only the 20 identified silica particles in each imaged field as shown in Figure 11). To measure the PSD of RCS particles, a manual on-screen method was used instead of the automated function in ImageJ, as the software cannot isolate a specific type of particle. The line tool in ImageJ was used to measure the length and width of RCS particles. The use of the line tool achieved more consistent measurements than

the ImageJ oval and freehand tools. Only independent and isolated RCS particles were selected, those that did not overlap with other mineral particles.

Additional RCS particle properties were then derived from the length and width measurements using mathematical equations (Sellaro et al., 2015).

a) The cross-sectional diameter (SEM dc) was calculated using Equation 3-1, following the calculation of the short dimension and maximum project sphericity (Sellaro et al., 2015):

- Short dimension (particle thickness), where the aspect ratio for quartz is R=0.7:

$$S = R \times W \qquad \text{Equation 3-1}$$

- Maximum projection sphericity (Ψp), which provides information about the shape of the particle, i.e. whether it is flat or spherical:

$$\Psi\rho = \sqrt[3]{\left(\frac{S^2}{L \times W}\right)} \qquad \text{Equation 3-2}$$

- Cross-sectional diameter (dc):

$$dc = \frac{L \times W}{2} \qquad \text{Equation 3-3}$$

b) The spherical diameter (SEM ds), which provides information about the aerodynamic nature of the particle, was calculated using Equation 3-4 (Sellaro et al., 2015):

$$ds = \Psi\rho \times L \qquad \text{Equation 3-4}$$

c) The spherical volume (SEM V), which is then calculated for the particle using Equation 3-5 (Sellaro et al., 2015):

$$V = \frac{4}{3}\pi\left(\frac{ds}{2}\right)^3 \qquad \text{Equation 3-5}$$

3.6.2 Using Laser Light Scattering (LLS) Analysis to Determine $PSD_{LLS(Dust)}$

The same dust sample that had been used for the SEM measurement was used to measure the PSD using the LLS ($PSD_{LLS(Dust)}$) method. The PSD of all the dust particles from the sample was measured according to ASTM C1070 (ASTM, 2014). However, the specimen used for the SEM analysis could not be removed from the sample stage as it was secured with double-sided tape. Removing it would tear the specimen and damage the sample. Therefore, the remainder of the same 25 mm diameter respirable dust filter sample was placed in a crucible with a liquid medium of 10 ml demineralised water. The crucible was placed in an ultrasonic bath for one to three minutes to remove all the dust from the filter membrane and suspend it in the liquid medium. The suspension was transferred to a fraction cell, the LLS sample holder (Figure 13) and placed in an LA Horiba 950 particle size instrument.

Figure 13: Fraction cell of the LLS instrument

The particle size from LLS was used to express the PSD as a function of volume, area, length and number. For the purposes of this study, LLS was undertaken using all four PSD expressions. In general, particle size by LLS analysis is expressed on a volume basis. Area, length and number are used as conversions for specific applications where methods are compared. The PSD where particle sizes are expressed on a number basis is used only when

comparing LLS to image analysis, which made the number distribution applicable to this study (Horiba, 2019).

The PSD is mathematically derived using the MIE theory (Horiba, 2007) and considers the refractive index of the dust sample. The refractive index is specific to the dust material and is a ratio of how the laser light is scattered by the dust material in a vacuum versus in a watery medium. The refractive index used in this study ranged between 1.54 and 1.59.

The data collection methods, SEM and LLS, were used to address Objective 1 (Section 3.7). The particle size results from Objective 1 were used to address Objective 2 (Section 3.8) and Objective 3 (Section 3.9) of this study.

3.7 Objective 1: Operationalising the SEM Method for Particle Sizing and Selection

To operationalise the RCS particle sizing, selection and effort on SEM, the methodology shown in **Error! Reference source not found.** was followed. Sections 3.7.1, 3.7.2 and 3.7.3 provide further detail.

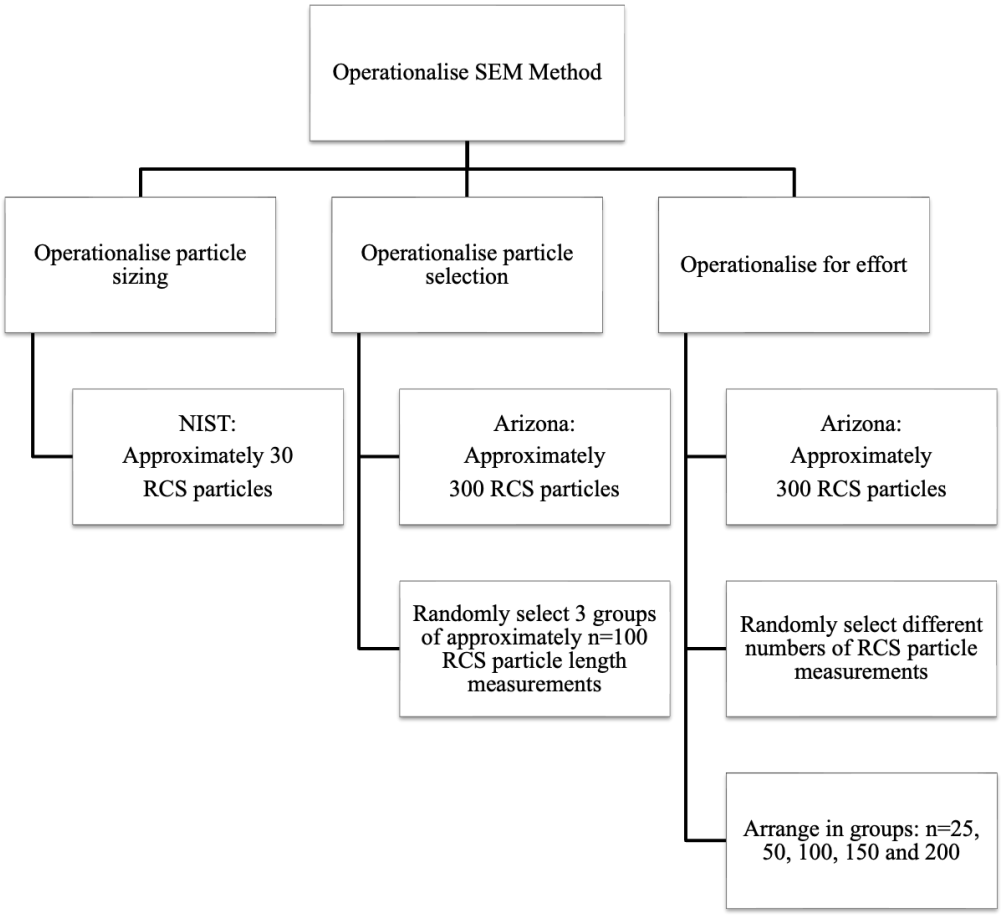

Figure 14: Process followed to operationalise the SEM method for RCS particle size measurements

3.7.1 Operationalise the particle sizing using SEM

Using the ImageJ sizing tools, the two-dimensional (2D) measurements of each particle were taken (i.e. length and width). In addition, using these measurements, additional particle-size properties were calculated for the particles, namely cross-sectional diameter (dc), spherical diameter (ds) and the particle volume (V). The RCS particle sizing was operationalised in a known standard reference dust material from NIST that consisted only of RCS particles.

3.7.2 Operationalise the particle selection using SEM for Arizona dust

Following the RCS particle sizing on the NIST standard reference material, the RCS particle selection was operationalised on sample of a mixture of dust. Arizona Ultra-Fine dust has a known composition and consists of RCS and non-RCS particles (Powder Technology, 2020).

The process to operationalise the RCS particle selection in a mixture of dust is shown in Figure 15. Only the RCS particle length measurements were used to operationalise the method for particle selection and not the additional particle size properties. The assumption was that, since the additional particle size properties were mathematically derived from the length measurements, they would be affected in the same manner by RCS particle selection as the length measurements.

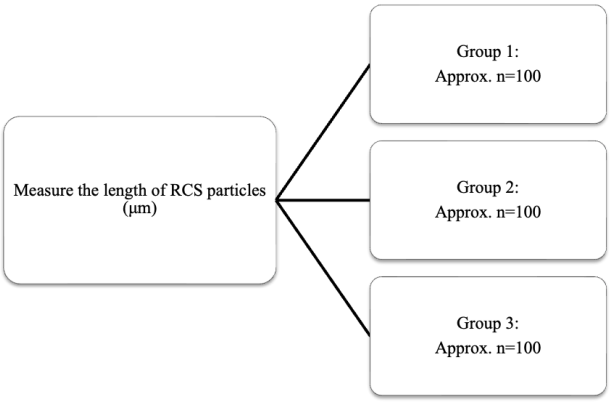

Figure 15: Process followed to operationalise RCS particle selection

Length measurements of approximately 300 RCS particles were taken and placed in three groups of approximately 100 and were compared to evaluate the repeatability of particle selection.

3.7.3 Operationalise the particle selection using SEM in terms of effort

Part of the process to operationalise the method for effort was to determine the smallest number of RCS particles to measure on one dust sample and maintain repeatability in terms of particle

selection. The SEM method is a time-consuming analysis, and minimising number of particles needed will assist in making the method more effective in the time available. RCS particle length was used for the repeatability test, as the subsequent, additional particle size properties were mathematically derived from the RCS particle length. The process followed is shown in Figure 16.

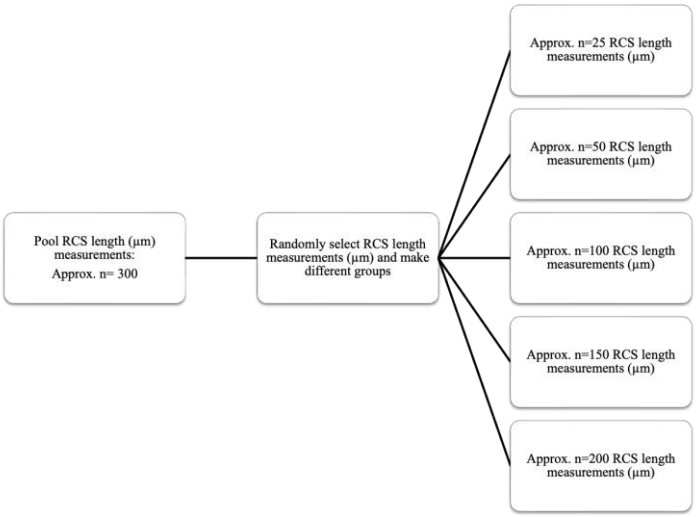

Figure 16: Process followed to operationalise the SEM method for effort

The length (µm) was measured on RCS particles on one Arizona sample. RCS length measurements were pooled and from this pooled data set (n=300), measurements were randomly selected and placed into five groups with different numbers of RCS particle length measurements, namely n=25, 50, 100, 150 and 200. The first 25 randomly selected measurements were removed and placed in the n=25 group; the second set of 50 randomly selected measurements, were placed in the n=50 group and so forth. The number of RCS particle size results in each set was decided by the researcher and was not prescribed by a standard.

3.8 Objective 2: Comparison of PSD LLS_{Dust} with PSD SEM_{Dust}

Objective 2 aims to determine whether a linear relationship exists between RCS PSD measurements on the same dust sample taken using the SEM and LLS methods, by using a simple linear regression model ($y = mx + c$). The RCS particle size obtained from SEM is the dependent variable (on the y-axis) and the particle size measurements for all dust particles obtained from LLS is the independent variable (on the x-axis).

The linear regression was derived using the D50 PSD parameter data of at least 10 samples where the LLS and SEM data were available for the same PSD metric. Table 3. shows all the particle size measurement metrics of the two methods.

Table 3.1: Particle size measurement metrics available for regressions

Notation	**Particle size measurement metric**	**Represents**
SEM (L)	SEM Length	RCS only (2D)
SEM dc	SEM Cross-sectional diameter (dc)	RCS only; Calculated from SEM (L)
SEM ds	SEM Spherical diameter (ds)	RCS only; Calculated from SEM (L)
SEM Vol	SEM Spherical volume (V)	RCS only; Calculated from SEM (L)
LLS Vol	LLS Distribution base: Volume	All dust particles (3D)
LLS Area	LLS Distribution base: Area	All dust particles (3D)
LLS Length	LLS Distribution base: Length	All dust particles (3D)
LLS Nr	LLS Distribution base: Number	All dust particles (3D)

The selected PSD metrics for comparison were volume, length and area (as shown Table 2.2). Regression models were fitted for each mineral matrix: NIST, Arizona and gold mine dust, respectively.

Table 2.2: Volume, length and area pairs for the regression models

Pair	LLS metric	SEM metric
Volume	LLS Vol	SEM Vol
Length	LLS Length	SEM Length
Area	LLS Area	SEM LxW

The agreement between the outcome of the different PSD metrics for SEM and LLS over the selected number of samples was determined using Wilcoxon rank sum test, also known as the Mann-Whitney (refer to Section 3.10.2).

3.9 Objective 3: Estimating the Particle Size of RCS from the SEM vs LLS Regressions

After comparing the particle size measurement results between the two methods using the Wilcoxon rank sum test, the linear regression for each mineral matrix was used for predictive analysis.

In practice, a laboratory usually only reports the D50 or median value of the cumulative particle size distribution. Accordingly, the D50-value (i.e. the median particle size) was used as the PSD parameter representing the RCS particle size in Objective 3.

The LLS D50-value was used to estimate the D50-value for RCS, and the outcome of the predictive analysis was compared to the D50-value for RCS measured using SEM to evaluate the accuracy of the estimation.

3.10 Data-analysis

The data-analysis methods outlined below were carried out using Microsoft Excel® for Mac, Version 16.69 (23010700), Stata Version 18.0 and JASP Version 0.18.3.

3.10.1 PSD parameters

PSD results are not one single value, but rather a probability density distribution over a size range. The number of actual particle size results varied for each area that was measured using the ImageJ software on SEM. The LLS method does not provide results showing an actual particle size per particle, but only a cumulative PSD, which can be captured in a number of cumulative distribution parameters, i.e. D10, D30, D50, D70 and D90:

- D10: 10% of all the PSD measurements were below this particle size in micron (μm).
- D30: 30% of all the PSD measurements were below this particle size in micron (μm).
- D50: 50% of all the PSD measurements were below this particle size in micron (μm). (The D50 is also known as the median value of the PSD measurements.)
- D70: 70% of all the PSD measurements were below this particle size in micron (μm).
- D90: 90% of all the PSD measurements were below this value or particle size in micron (μm).

Most of the comparisons between the two methods (LLS and |SEM) are done with the D50 of the PSD.

3.10.2 Wilcoxon rank sum test (Mann-Whitney)

The LLS and SEM data sets were tested for normality using the Shapiro-Wilk test (Shapiro and Wilk, 1965). This test was applied to determine whether the values in the data set were normally distributed despite any outliers or a wide variance among the values. The normality test was done prior to the Wilcoxon rank sum (Mann & Whitney, 1947) and Kruskal-Wallis tests in Objective 2.

The Wilcoxon rank sum (Mann-Whitney) test was applied to compare the LLS with the SEM measurements e.g. volume, length and area. Although the PSD metrics were paired (i.e.,

volume, length and area), the particle size data by LLS and SEM are independent from one another because SEM measures individual particle size but LLS measure the PSD of all particles in the sample.

3.10.3 ANOVA and Kruskal-Wallis

The Analysis of Variance (ANOVA) (Ross & Willson, 2017) was used to determine whether there was a difference in the mean values of different sets of results. ANOVA compares the means of two or more groups for one dependent variable (Ross & Willson, 2017).

General requirements for ANOVA are that each group (n=100 each) has a normal distribution, similar variances and independent samples were drawn by random selection (Illowski & Dean, 2013). A formal test for normality was done using Shapiro-Wilk. If the assumptions for ANOVA were not met, the Kruskal-Wallis was applied (Kruskal & Wallis, 1952).

One-way ANOVA was applied in Objective 1 to determine if there was a significant difference in the median D50-values from three different groups that each contain 100 RCS particle length measurements obtained by three different drawing tools.

To determine if there was a difference between the groups that contain different number of RCS particle size measurements i.e., n=25, 50, 100, 150 and 200, Kruskal-Wallis was applied and Dunn’s multiple comparison post-hoc tests (Dunn, 1961) were conducted to further analyse differences between the medians of the particle number groups groups.

3.10.4 Bland-Altman Plots

To investigate a possible structural bias between the different SEM drawing tools (relevant to Objective 1) i.e. line, freehand and oval tools, the particle size measurements were compared using a Bland-Altman plot (Bland & Altman, 1995). The Bland-Altman (B-A) plot is a scatter plot of the mean differences between two measurement results from two drawing tools. A

horizontal line is also included on the plot, representing the mean difference between the two tools’ measurements. The plot also typically includes lines that represent 1.96 standard error of the differences, from the mean difference (mean ± 1.96 SE), which was used to determine whether the differences over the observed range indicated a systematic bias.

3.10.5 Linear Regression Analysis

Linear regression analysis was conducted to predict the PSD parameter D50-values based on SEM from the LLS PSD D50-values (Objective 2). The linear regression is expressed as $y = mx + c$, where y represents the dependent value (SEM D50-value), m is the slope of the regression, x is the independent variable (LLS D50-value) and c is the point where the x-axis intercepts the y-axis. When the regression line has a y-intercept value, the associated value is $x=0$.

To address Objective 3, the regression models obtained for Objective 2 were applied, and the predicted SEM_{RCS} D50-value was compared with the actual D50-values measured by SEM_{RCS}.

Chapter 4: Results

4.1 Introduction

This chapter presents the results of this study in line with the objectives of the study; its flow depicted in Figure 17.

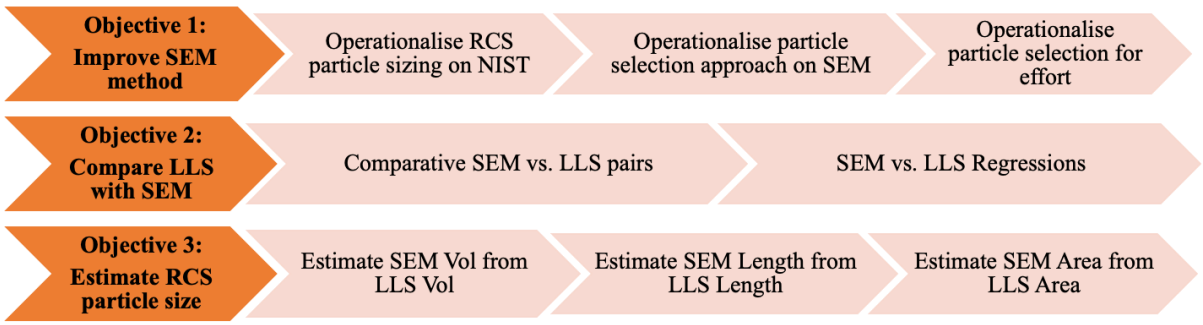

Figure 17: Flow of the study for achieving the results in line with the study objectives

4.2 Objective 1: Operationalise the SEM Method for RCS Particle Sizing and Selection

The first objective of the study was:

> To operationalise the Scanning Electron Microscopy (SEM) method for accuracy and effort in measuring the particle size in respirable dust samples of NIST, Arizona, and gold mine dust, through the selection, the number of individual particles to be analysed and the accurate sizing of these particles.

Figure 18 shows a graphical representation of the methodology that was followed to achieve Objective 1.

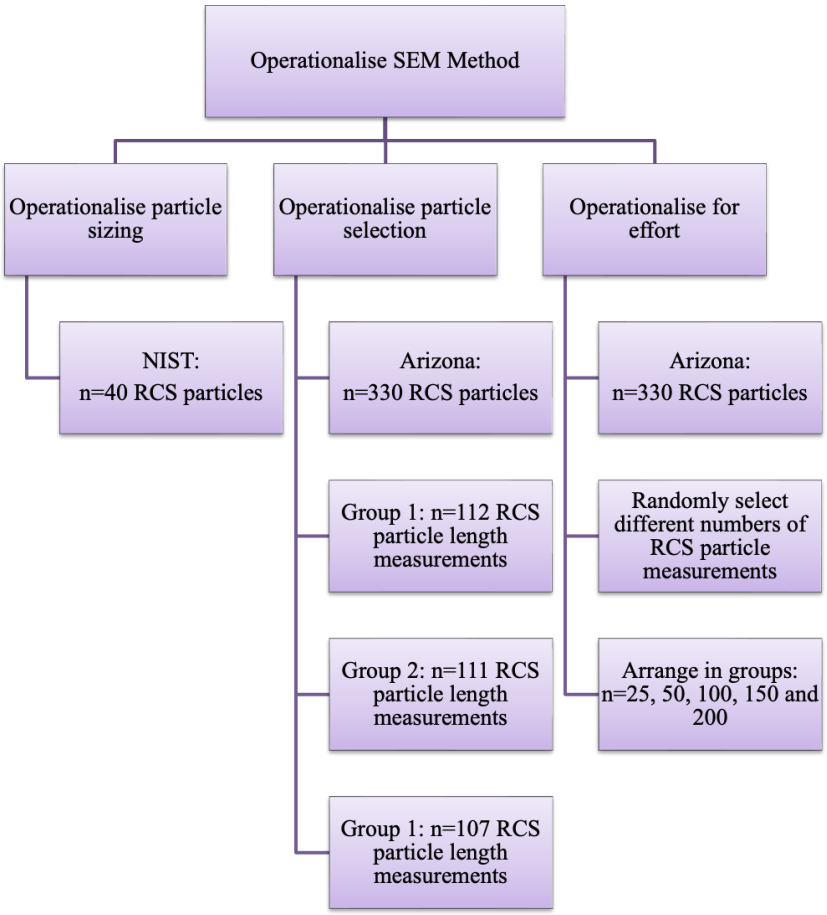

Figure 18: Overview of the methodology for Objective 1

4.2.1 Operationalise the SEM Method for Particle Sizing on NIST SRM (pure silica)

The particle size measurements from three ImageJ drawing tools were compared on one archived sample of the NIST SRM:

- Freehand tool: measures the irregular perimeter of the RCS particle using freehand drawing.
- Line tool (linear) tool: measures the longest dimension of the RCS particle in a straight line.
- Oval (circular) tool: measures the circumference by adjusting an oval shape over the RCS particle.

One analysis area (288 x 159 µm) was selected, and 10 RCS particles were selected and measured manually using the three tools.

Figure 19 shows a comparison of the particle sizes as determined the three drawing tools.

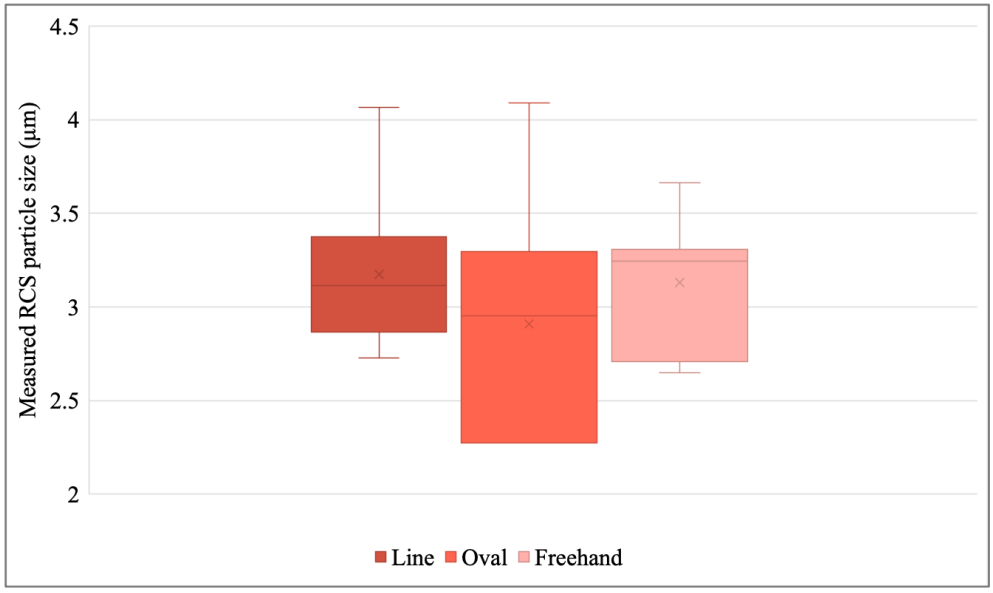

Figure 19: Comparison of the particle size results obtained from three ImageJ drawing tools

Bland-Altman plots (Bland & Altman, 1995) was used to determine the mean difference among the three drawing tools (i.e., Freehand *vs.* Line and Oval *vs.* Line). Figure 20 and Figure 21 show the mean differences that fall within the 95% confidence interval (greyish purple area) and the mean differences that fall within the ± 1.96 standard error (green and orange shaded areas). The mean differences between the Line drawing tool and the other two tools, were similar i.e., six and five observations within the 95% confidence interval respectively.

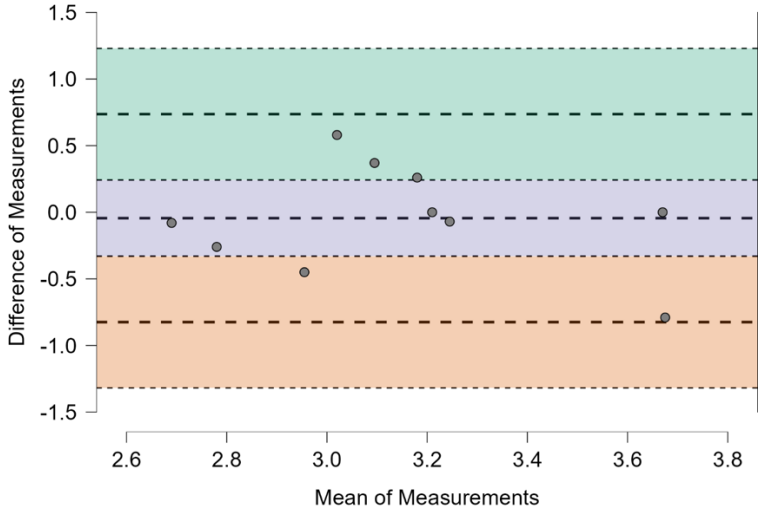

Figure 20: Mean differences between Line and Freehand drawing tools

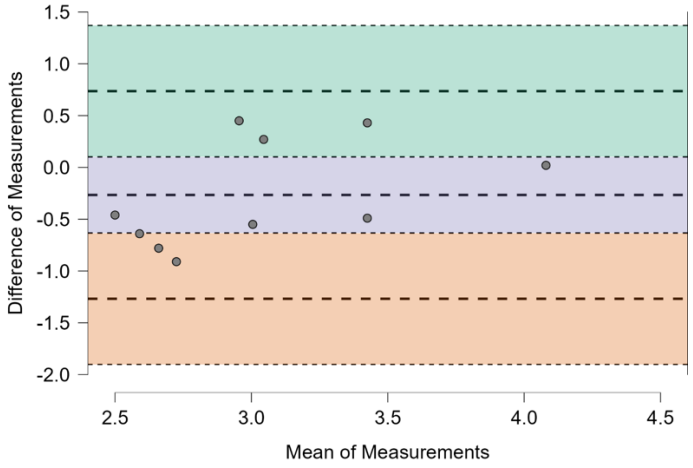

Figure 21: Mean differences between Line and Oval drawing tools

To calculate the additional particle properties on the same RCS particles, hence obtaining various PSD metrics, the cross-sectional diameter (dc), spherical diameter (ds) and spherical volume (V), the Sellaro et. al. (2015) mathematical equations were used. Figure 22 shows the particle size distributions for the same set of RCS particles expressed for different PSD metrics.

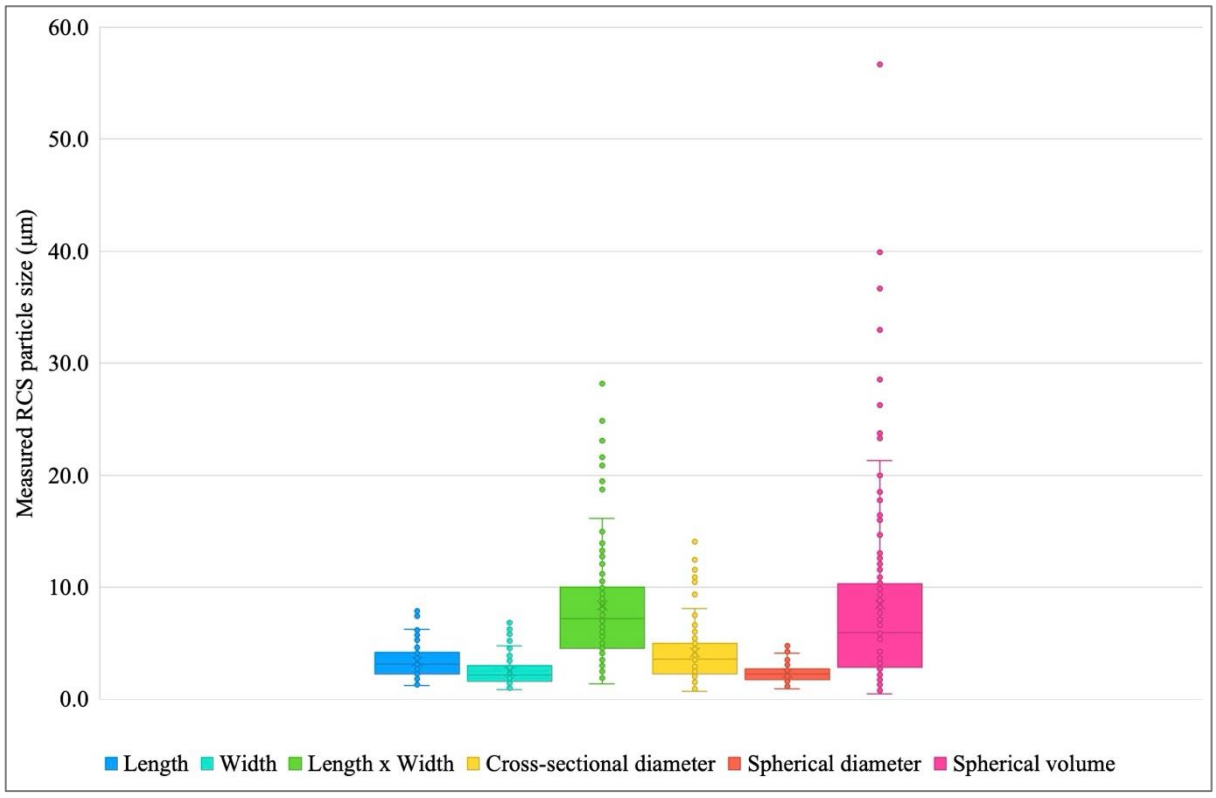

Figure 22: Particle size distributions for the same set of RCS particles expressed for different PSD metrics

Given that the additional particle characteristics are based on the measured length and width dimensions of the RCS particles, it was decided to continue with the line drawing tool only.

The D50-value of the NIST according to the CoA is 1.6 µm, but none of the drawing tools or calculations provided that same D50-value.

Although it was not part of the original protocol, the RCS particle sizing was also operationalised on mixtures of dusts, namely Arizona dust and gold mine dust. The reason for

going beyond the original protocol was to determine if the sizing would be different in a mixture of dust. It was found that the RCS particle size distribution was not different in a mixture of dust when compared to NIST. Refer to the Appendix 4 for the detailed results.

The material safety data sheet (MSDS) for the Arizona dust shows that the D50 is between 2.75 and 5.50 μm, as determined using LLS. The RCS particle size results (dc, ds and V) compared well with the PSD results on MSDS, with the D50s being 3.38 μm, 2.25 μm and 5.93 μm, respectively (refer to Appendix 4).

The spherical diameter (ds) and cross-sectional diameter (dc) results for the gold mine dust showed promise because the D50s were 2.09 μm and 3.19 μm, respectively. These particle sizes would be anticipated from real-world, personal-exposure samples with a size range of less than ± 10 μm (refer to Appendix 4).

4.2.2 Operationalise the particle selection approach on SEM

The RCS particle selection was assessed using one Arizona dust sample. Figure 23 shows an overview of the process that was followed:

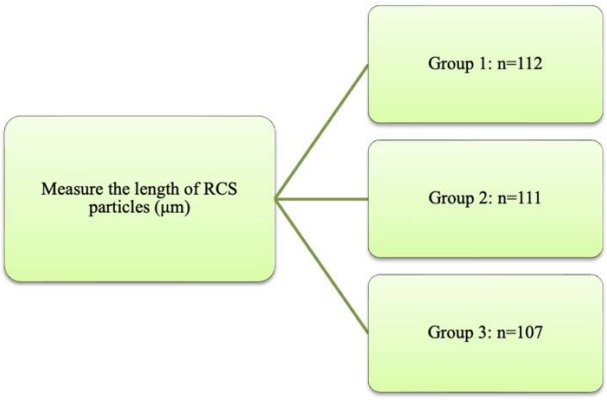

Figure 23: Process followed for particle selection in Arizona dust

A total of 330 RCS particle size length measurements were taken and arranged in three different groups, namely, Group 1 (n=112, 1st 112 measurements), Group 2 (n=111; 2nd 111 measurements) and Group 3 (n=107; 3rd 107 measurements). SEM mapping was used to distinguish RCS from other mineral dust particles. RCS particles are coloured yellow in Figure 24.

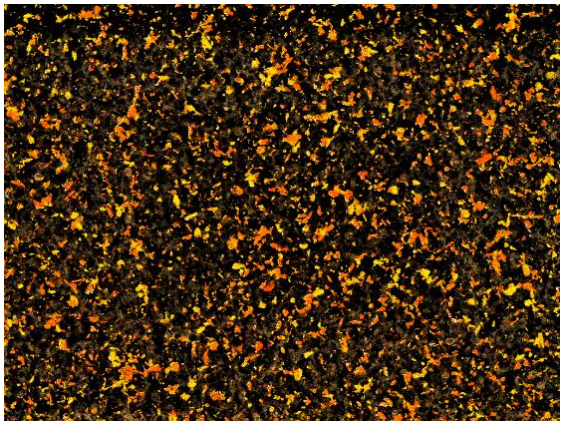

Figure 24: SEM mapping using different colours to distinguish RCS particles (yellow)

Energy-dispersive X-ray spectroscopy (EDS) was used to confirm that the elemental composition of the particle was SiO_2, as the interest was only in RCS particles (refer to Figure 25).

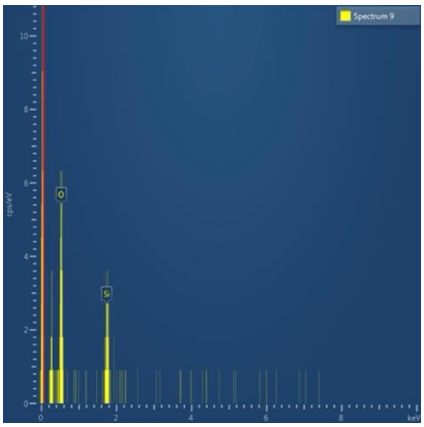

Figure 25: EDS analysis confirming that the composition of the particle is SiO_2

Refer to Figure 26 for a comparison between the results from the three groups and the pooled results. The RCS particle length measurements between the three groups were compared using the one-way ANOVA and statistically significant differences were observed (p=0.002)

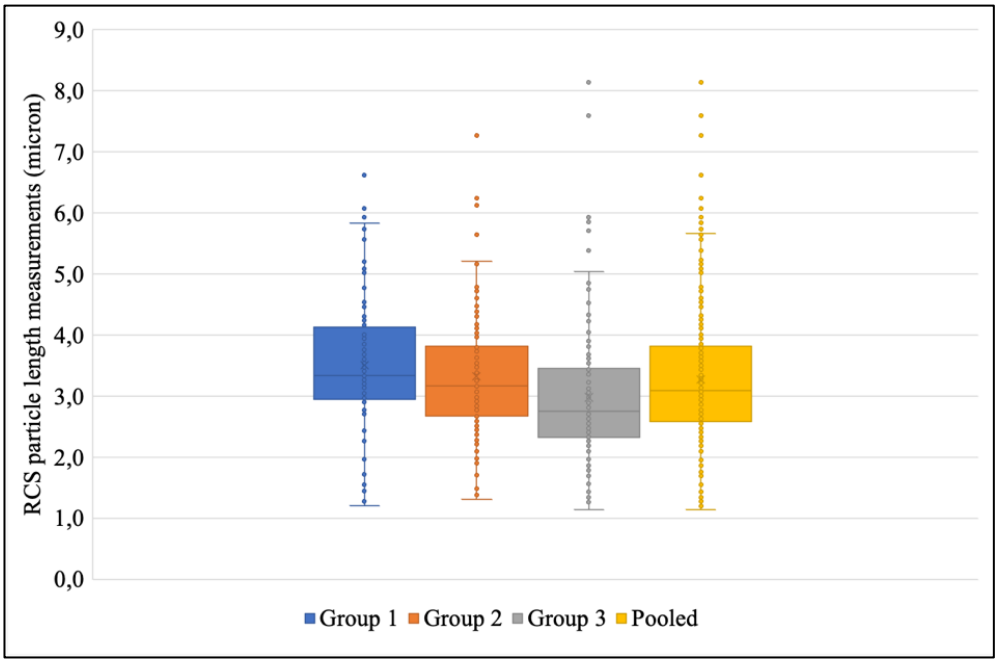

Figure 26: Comparison of the RCS particle length measurements for four groups

4.2.3 Operationalise the Particle Selection for Effort

The methodology was assessed for effort to determine finding the minimum number of RCS particles that need to be measured to maintain the repeatability of RCS particle selection. Different numbers of RCS particles were randomly selected in five groups, viz. n=25, n=50, n=100, n=150 and n=200, from a total of n=330 RCS particle measurements. The number of RCS particle size results in each set was decided by the researcher and was not a prescriptive number.

The particle selection was repeated several times, and in total seven samples (representing each the five particle size groups) were statistically analysed using the free software package JASP Version 0.18.3 (https://jasp-stats.org/). The non-parametric Kruskal-Wallis and Dunn’s

multiple comparison post-hoc tests were used to demonstrate a difference between the group medians.

Testing the medians of five groups of particle numbers in RCS particle length measurements for seven samples revealed no systematic differences between specific particle number groups (Table 4.1).

Table 4.1 Results of Kruskal-Wallis test for seven random samples consisting of five groups of particle numbers (N=25, N=50, N=100, N=150, and N=200) taken from a population of 330 analysed particles

Sample	K-W (p-value)	Dunn's post hoc
1	0.131	Not appropriate
2	0.017	A significant difference between group N=100 and the groups N=150 and N=200
3	0.100	Not appropriate
4	0.082	A significant difference between groups N=50 and N=150
5	0.659	Not appropriate
6	0.696	Not appropriate
7	0.383	Not appropriate

During the execution of this objective, it was discovered that simulations and sensitivity tests would be required to find the “true” minimum number of RCS particles that could be measured to improve the SEM method for effort because many factors may influence the minimum number required (e.g. dust load, mineral composition or conductivity, to name a few factors). The extent of the work required to determine the minimum number of RCS particles to be measured was not within the scope of this study; therefore, it was not further investigated. Sellaro et. al. was used for guidance, where 100 particles were analysed on three samples. To compare the PSD results between the SEM and the LLS methods, leading practice of Sellaro

et. al. was followed and a selection of approximately 100 individual RCS particles was deemed sufficient to reach the objectives of this study. (It is acknowledged that the number of particles must be reviewed for future studies that involve real-world dust samples from different workplaces).

The archived samples were inspected to select at least ten samples in total, representing three mineral dusts (NIST, Arizona and goldmine). There were 25 potential samples but only 12 samples could be used for the study. The dust loads of six samples were too low for reliable LLS analysis because the laser transmission on the LLS analysis was more than 90% (i.e. not enough particles to scatter the laser light and derive a size distribution). Seven SEM specimens from filters were not sufficiently conductive, despite repeated carbon-coating to improve conductivity. The lack of conductivity resulted in a blurry and grainy image, with the result that individual particles could not be distinguished from one another. The lack of conductivity was not related to the mineral matrix or the type of membrane filter (i.e. MCE, PVC or silver). The reason for the lack of conductivity was not further explored and was outside the scope of the study. The outcome was that 12 out of 25 samples had a sufficient dust load and conductivity for further analysis, and two sets of data for both LLS and SEM. The samples were four NIST, five Arizona, and three goldmine dust samples, and within the time and budget constraints, no further samples were analysed.

4.2.4 Summary of Results from the operationalisation of the SEM Method

In assessing the ImageJ software drawing tools, the line drawing tool was found to be more useful in obtaining PSD measurements. The line tool was used to measure the length and width of the RCS particles, and from these measurements, the additional measurements were calculated.

SEM mapping was used to distinguish RCS and non-RCS particles from one another by using different colours. The mapping made the manual measurements of the RCS particles accurate and effective, and a large number of particles were measured in a short time (e.g. more than 20 particles in approximately 20 minutes).

When the particle selection was assessed, the results showed that the PSD measurements were not dependent on the area from which the particles were selected. This outcome was positive, as the measured specimen must represent the entire sample.

The first objective was to operationalise the SEM for effort by finding the minimum number of RCS particles that need to be measured. Within the scope of this study, the minimum number could not be accurately determined, but approximately 100 RCS particles were shown to be sufficient to compare the PSD results obtained between two methods.

4.3 Objective 2: Comparison of $PSD_{LLS(Dust)}$ with $PSD_{SEM(RCS)}$

The second objective of the study was:

> To compare the particle size distribution (PSD) results attained by Laser Light Scattering (LLS) with the particle size results achieved by Scanning Electron Microscopy (SEM) to show the relationship between the results obtained by the two methods.

4.3.1 PSD metrics used for the SEM *vs.* LLS regressions

The same filters that were used for SEM analysis were used for LLS analysis. The D50-value of the LLS results for each of the three distribution bases were used: volume, length and area. The PSD metrics for the SEM results were compared with the LLS metrics in this section.

To achieve Objective 2 the process outlined in Figure 27 was followed.

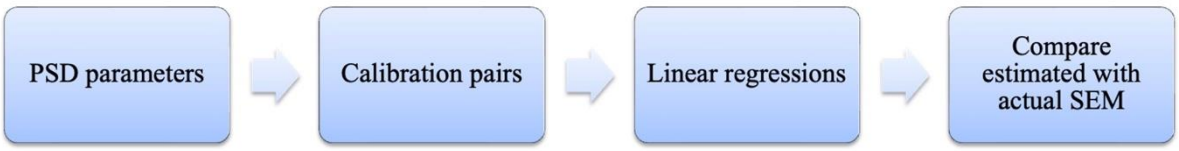

Figure 27: Process followed to achieve Objective 2

The same filters used for SEM analysis were used for LLS analysis, and the D50 (median) of the size distribution was reported. Table 4.2 shows all the D50 of the RCS particle size measurements (µm) of the 12 samples for four different PSD metrics.

Table 3.2: D50-values (µm) of dust particle size distributions using LLS, and the D50-values for RCS particle size distributions using SEM (µm) for different PSD metrics

Sample Nr	Matrix	LLS Area	LLS Length	LLS Nr	LLS Vol	SEM (L)	SEM dc	SEM ds	SEM Vol	SEM LxW
S02	Arizona	0.39	0.25	0.21	5.33	3.34	3.38	2.25	5.93	6.76
S05	NIST	0.18	0.15	0.15	8.61	3.17	3.59	2.25	5.98	7.18
S07	Arizona	6.16	4.87	3.60	8.05	4.26	6.83	3.03	14.56	13.65
S08	Arizona	0.15	0.13	0.12	7.26	4.42	6.70	3.05	14.83	13.39
S09	Arizona	0.21	0.25	0.16	8.23	3.57	4.51	2.50	8.22	9.03
S10	Gold mine	3.42	0.40	0.27	5.35	4.08	5.01	2.70	10.36	10.03
S11	Gold mine	0.20	0.17	0.09	6.12	4.07	5.87	2.90	12.83	11.74
S13	NIST	0.18	0.15	0.14	7.89	3.95	6.71	2.89	12.69	13.41
S15	Gold mine	0.15	0.13	0.13	3.34	3.73	5.26	2.69	10.17	10.52
S16	NIST	0.18	0.16	0.15	2.38	3.93	6.08	2.87	12.32	12.15
S17	NIST	1.93	0.23	0.18	26.91	3.91	5.85	2.80	11.47	11.70
S18	NIST	1.87	0.29	0.31	2.44	4.14	6.78	3.15	16.42	13.56

It is acknowledged that the LLS Area, Length and Nr measurements are an order of magnitude smaller than the respirable range (less than ten micron). These values were derived from the LLS Vol using the instrument’s software algorithm. The algorithm is a mathematical

conversion and uses information not available to the instrument user e.g. light detected in each of the 93 channels).

4.3.2 SEM *vs.* LLS comparison

The results for the same PSD metric obtained by LLS and SEM per sample that were used per regression for NIST, Arizona and goldmine dust, are reported. The D50 PSD values from Table 4.2 for the selected PSD| metrics, i.e. volume, length and area diameter, were rearranged according to the detection methods. Each data set for each method was tested for normality using the Shapiro-Wilk test as shown in Table 4.3. None of the LLS data sets were normally distributed (p-value < 0.05) whereas there was insufficient evidence of non-normality within the SEM data sets (p > 0.05).

Table 4.3: D50-values of the particle size measurements for SEM and LLS metrics (µm) for volume, length and area

Sample Nr	LLS Vol	SEM Vol	LLS Length	SEM (L)	LLS Area	SEM LxW
S02	5.33	5.93	0.25	3.34	0.39	6.76
S05	8.61	5.98	0.15	3.17	0.18	7.18
S07	8.05	14.56	4.87	4.26	6.16	13.65
S08	7.26	14.83	0.13	4.42	0.15	13.39
S09	8.23	8.22	0.25	3.57	0.21	9.03
S10	5.35	10.36	0.40	4.08	3.42	10.03
S11	6.12	12.83	0.17	4.07	0.20	11.74
S13	7.89	12.69	0.15	3.95	0.18	13.41
S15	3.34	10.17	0.13	3.73	0.15	10.52
S16	2.38	12.32	0.16	3.93	0.18	12.15
S17	26.91	11.47	0.23	3.91	1.93	11.70
S18	2.44	16.42	0.29	4.14	1.87	13.56
p-value (Shapiro-Wilk)	<0.001	0.656	<0.001	0.644	<0.001	0.121

The median and the inter-quartile range (i.e. 25th to 75th percentile), are shown in Table 4.4. The median values were compared using the Wilcoxon rank sum test. There are significant differences between the median D50-values of LLS and SEM for the PSD metric pairs volume, length and area ($p < 0.05$).

Table 4.4: Comparison between the medians of the D50-values for the LLS and SEM method

PSD Metric	PSD Method	Median of the D50-values (µm) (Inter-Quartile Range (IQR))	Exact probability (p-value Wilcoxon rank sum test)
Volume	LLS Vol	6.69 (4.34 – 8.14)	0.007
	SEM Vol	11.90 (9.20 – 13.70)	
Length	LLS Length	0.2 (0.15 – 0.27)	< 0.001
	SEM (L)	3.94 (3.65 – 4.11)	
Area	LLS Area	0.20 (0.18 – 1.90)	< 0.001
	SEM LxW	11.72 (9.52 – 13.40)	

4.3.3 SEM *vs.* LLS regressions

Regression models were fitted with the D50 from the SEM as the outcome variable and the D50 from the LLS for the same sample as the explanatory variable. Table 4.5 shows the regressions and their significance.

Table 4.5: Regressions coeficients for the three PSD metrics

PSD Metric	Regression slope β (95% Confidence Interval)	p-value
Volume	-0.04 (-0.40 – 0.32)	0.812
Length	0.09 (-0.09 – 0.27)	0.300
Area	0.42 (-0.45 – 1.29)	0.390

The results presented in Table 4.5 show that the models does not significantly predict the response variable SEM [(β range -0.04 to 0.42)], all p > 0.30], meaning that the regression models show that a unit change in the LLS value does not result in a significant unit change in the estimated SEM_{RCS}.

4.4 Objective 3: Estimation of the Particle Size of RCS from the SEM: LLS regressions

The third objective of the study was:

> To estimate the particle size of respirable crystalline silica (RCS) from $PSD_{LLS(Dust)}$ in an unknown dust sample and compare the estimated results with measured data ($PSD_{SEM(RCS)}$).

The three regression models were used to estimate SEM_{RCS} from the LLS_{Dust} values and the estimated SEM_{RCS} values were compared with the actual SEM_{RCS}.

4.4.1 Estimated SEM Vol from LLS

Table 4.6 compares the actual SEM_{RCS} with the estimated SEM_{RCS} using the regression model for Volume: $SEM_{RCS} = 11.62 – 0.04\ LLS_{Dust}$, (from Table 4.5).

Table 4.6: Actual vs. estimated SEM_{RCS} Volume of the D50-values

Sample Nr	Mineral matrix	LLS Vol (µm)	Actual SEM Vol (µm)	Estimated SEM Vol (µm)	Residual error
S02	Arizona	5.33	5.93	11.41	-5.48
S05	NIST	8.61	5.98	11.28	-5.30
S07	Arizona	8.05	14.56	11.30	3.26
S08	Arizona	7.26	14.83	11.33	3.50
S09	Arizona	8.23	8.22	11.29	-3.07
S10	Gold mine	5.35	10.36	11.41	-1.04
S11	Gold mine	6.12	12.83	11.38	1.45
S13	NIST	7.89	12.69	11.31	1.39
S15	Gold mine	3.34	10.17	11.49	-1.31
S16	NIST	2.38	12.32	11.53	0.80
S17	NIST	26.91	11.47	10.55	0.92
S18	NIST	2.44	16.42	11.52	4.89

There was not sufficient evidence that the residual error between the actual and estimated SEM_{RCS} departed from a normal distribution (Shapiro-Wilk $p = 0.54$). The regression satisfies the test normality and the basic assumptions that were made.

4.4.2 Estimated SEM Length from LLS

Table 4.7 compares the actual SEM_{RCS} with the estimated SEM_{RCS} using the regression model for Length: $SEM_{RCS} = 3.83 + 0.09\ LLS_{Dust}$ (from Table 4.5).

Table 4.7: Actual vs. estimated SEM_{RCS} Length of the D50-values

Sample Nr	Mineral matrix	LLS Length (µm)	Actual SEM (L) (µm)	Estimated SEM (L) (µm)	Residual error
S02	Arizona	0.25	3.34	3.85	-0.51
S05	NIST	0.15	3.17	3.84	-0.67
S07	Arizona	4.87	4.26	4.26	0.00
S08	Arizona	0.13	4.42	3.84	0.58
S09	Arizona	0.25	3.57	3.85	-0.28
S10	Gold mine	0.40	4.08	3.86	0.22
S11	Gold mine	0.17	4.07	3.84	0.23
S13	NIST	0.15	3.95	3.84	0.11
S15	Gold mine	0.13	3.73	3.84	-0.11
S16	NIST	0.16	3.93	3.84	0.09
S17	NIST	0.23	3.91	3.85	0.06
S18	NIST	0.29	4.14	3.85	0.29

There was not sufficient evidence that the residual error between the actual and estimated SEM_{RCS} departed from a normal distribution (Shapiro-Wilk $p = 0.71$). The regression satisfies the test normality and the basic assumptions that were made.

4.4.3 Estimated SEM Area from LLS

Table 4.8 compares the actual SEM_{RCS} with the estimated SEM_{RCS} using the regression model for Area: $SEM_{RCS} = 10.57 + 0.42\ LLS_{Dust}$ (from Table 4.5).

Table 4.8: Actual vs. estimated SEM_{RCS} Area of the D50-values

Sample Nr	Mineral matrix	LLS Area (µm)	Actual SEM LxW (µm)	Estimated SEM LxW (µm)	Residual error
S02	Arizona	0.39	6.76	10.74	-3.97
S05	NIST	0.18	7.18	10.65	-3.46
S07	Arizona	6.16	13.65	13.14	0.51
S08	Arizona	0.15	13.39	10.63	2.76
S09	Arizona	0.21	9.03	10.66	-1.63
S10	Gold mine	3.42	10.03	12.00	-1.97
S11	Gold mine	0.20	11.74	10.65	1.08
S13	NIST	0.18	13.41	10.65	2.77
S15	Gold mine	0.15	10.52	10.63	-0.11
S16	NIST	0.18	12.15	10.65	1.51
S17	NIST	1.93	11.70	11.38	0.32
S18	NIST	1.87	13.56	11.35	2.21

There was not sufficient evidence that the residual error between the actual and estimated SEM_{RCS} departed from a normal distribution (Shapiro-Wilk $p = 0.36$). The regression satisfies the test normality and the basic assumptions that were made.

4.5 Summary of the results from the estimation of the particle size of RCS from the SEM *vs* LLS regressions

Regression models were obtained for the three SEM and LLS pairs, volume, length, and area, and there was insufficient evidence to conclude that the underlying distribution was not normal ($p > 0.05$). Despite this outcome, the estimated SME values for volume, length, and area were significantly different from the actual SEM values. This means that LLS is not a good predictor of SEM_{RCS}, and other approaches must be explored.

Chapter 5: Discussion

5.1 Introduction

The results of the study are discussed in line with each study objective.

5.1.1 Objective 1: Operationalise the SEM method for particle sizing and selection

The SEM method was operationalised for accuracy and effort by ensuring that the particle sizing, selection and number of individual particles to be analysed were accurate.

In practice, laboratories conduct PSD analysis more often on samples with a mixed composition of dust than on samples of pure silica. Under these conditions, the manual sizing tools are useful for measuring the PSD of RCS particles, and the mathematical derivation of the additional PSD properties (cross-sectional and spherical diameter, and volume) from the SEM length and width measurements.

An interesting finding was that the actual values of the RCS length, width, spherical, cross-sectional and volume of the particles varied over a wide range. The RCS length and width are based on the 2D measurement of the RCS particle whereas the spherical diameter, cross-sectional diameter and volume were derived mathematically. In essence, the values obtained from these metrics provided different perspectives on the same RCS particle, hence the differences in the actual values. The dimensions of the particles are described by the different PSD metrics and provides useful information when dust particles are characterised (Hegel et al., 2014).

The SEM method was improved for selection in a dust where RCS and non-RCS particles were mixed. The manual measurement of the PSD of RCS particles was found to be an effective and affordable methodology (i.e. 20 particles could be measured in 20 minutes). Although an automated method to measure the size of all dust particles was tested, this approach does not

distinguish the RCS from the non-RCS particles. Only the manual measurement method was used further in the study.

Sellaro et al. (2015), Johann-Essex et al. (2017) and Sarver et al. (2019) characterised the composition of coal mine dust using SEM. The authors determined the particle number distribution of the different mineral constituents contained in the dust i.e., the number of particles with the same elemental composition. Although the concentration of crystalline silica in relation to the other constituents was determined, the intent of these studies was not to measure RCS particle size in the dusts. However, Sarver et al (2021), Keles et al (2022), and Animah et al (2024) went further to determine the PSD of RCS using SEM in relation to the PSD of the other minerals in the dust. Keles et al (2022) found that it was difficult to measure RCS particles that were partially covered with other non-RCS particles due to high dust load.

A point of concern is that the manual method for measuring RCS particles depends heavily on the discretion and subjectivity of the analyst. In practice, an analyst may prefer to select bigger, more visible particles or opt to select particles from one small area only (e.g. 228 x 159 µm image area). To determine the sensitivity of the SEM method to particle selection, the SEM length of RCS particles was measured on five areas of the Arizona (mixed-dust) sample. No statistically significant differences were found, which was a positive outcome for future analyses. This means that SEM-EDS mapping and colour coding greatly assist with selecting RCS particles, confirming the approach taken by Sellaro et al. (2015). This outcome means that, in practice, a specimen can be taken from a mixed dust, and the RCS particles can be measured in any area.

The intent was to further operationalise the SEM method in an effort to maintain the quality and repeatability of the method. Different numbers of RCS particles were randomly selected in five groups, viz. n=25, n=50, n=100, n=150 and n=200, from a total of n=330 RCS particle

measurements. The particle selection was repeated several times, and in total seven selection samples were compared. Overall, no statistically significant difference was found in the groups, ($p > 0.082$). A significant difference was found for group n=100 when compared with the groups n=150 and n=200 ($p = 0.017$).

Sellaro et al. (2015) measured 100 RCS particles from three samples and for the purposes of the comparison between LLS and SEM, the measurement of 100 RCS particles per dust sample was deemed sufficient for this study.

In further studies Sarver et al. (2019) characterised 250 to 300 particles to obtain a detailed analysis of coal mine dust from eight Appalachia mines. In practice, a laboratory will follow a method validation process (SANAS, 2017) and part of this process will be to determine the minimum number of particles to measure to ensure that the method is fit for the intended purpose (ISO, 2017).

5.1.2 Objective 2: Comparison of $PSD_{LLS(Dust)}$ with $PSD_{SEM(Dust)}$

The D50-values of the PSD established by LLS were compared with the D50-values in the particle size distribution as measured by SEM using PSD metrics volume, length and area. The median values of the D50-values PSD for the PSD metrics were significantly different.

To achieve objective 2, the intention was to create a robust regression model using all three mineral dusts. In an ideal setting, a linear relationship should support accurate estimations of SEM_{RCS} from LLS_{Dust} measurements. Three regression models were derived based on the PSD metrics volume, length and area, but the slope of each regression model was non-significant. LLS_{Dust} did not provide accurate estimations for the SEM_{RCS} and cannot be used as a reliable predictor.

In a real-world setting, when analysing dust with an unknown composition, a linear relationship may not be the best model to fit and alternatives may be explored. When LLS *vs.* SEM regression models are considered in future for samples with a complex mineral matrix, non-linear regressions may be worth exploring to determine if they are fit for the intended purpose. During a comprehensive method validation process, the LLS *vs.* SEM regression may be improved so that the estimated SEM_{RCS} is as close as possible to the measured $SEM_{RCS.}$

Comparisons between SEM and LLS methods have been done in other studies. Hegel et al. (2014) compared laser diffraction with SEM using poly-vinyl chloride resin-based compound. Grubbs et al. (2021) also compared laser diffraction with SEM using powder-based additives. The authors concluded that each method provides useful and supplementary data about the material being analysed and agreed that variability in the PSD can be expected. The objectives of the two studies above were not to compare the two methods but to use the information from the two methods to characterise an elemental compound. Despite the fact that different minerals were used, these authors also observed that there were significant differences in the actual values obtained between SEM and LLS.

The differences between the actual D50-values obtained from the SEM and LLS PSDs were quite considerable for all dust types (NIST, Arizona and gold mine dust). This difference was an unexpected finding, considering that the NIST sample was made of pure silica and had not been mixed with other mineral dusts. For example, the median D50-values for volume, length and area obtained by LLS for NIST was 0.29 µm and for SEM was 11.47 µm. The MSDS presented a median value of 1.6 µm and was determined using LLS, and not SEM (NIST, 2005).

Hegel et al (2014) found that higher variations in the SEM PSD are more likely at small particle sizes. The mineral dust samples used in this study had particle sizes less than ten microns,

which may explain the variation in actual values between SEM and LLS. The smaller the particle size of RCS, the higher the risk of analysts’ manual measurement errors on SEM.

Differences in the principles of both PSD detection methods could further explain the actual differences between the SEM and LLS PSD results. SEM is a surface analysis method, and the measurements are done in 2D, i.e. the actual length and width of individual RCS particles, and the cumulative size distribution is calculated. LLS measures all dust particles in 3D, from different angles and uses a mathematical algorithm to calculate the PSD. The different principles in PSD measurements created uncertainty around what is the ‘true’ particle size of RCS. The SEM method is the ‘gold standard’ because SEM-EDS can firstly identify each individual particle is RCS based on the elemental composition (as opposed to non-RCS particles), and secondly it can measure the individual particle size of RCS particles with precision (ISO, 2011).

In this study, the actual median D50-values based on the volume, length and area obtained by SEM were much higher than those obtained by LLS. This could be due to a selection bias, since the LLS lower size range of detection was 0.13 μm (LLS Length), but the lowest size of the selected particles for SEM analysis appeared to be 3.17 μm (SEM Length). A higher magnification on SEM might enable the visual detection of smaller particles or those below the interaction volume for SEM. The LLS sample preparation uses ultrasonication to loosen dust particles from the membrane filter and therefore LLS may be possible to detect smaller particles. The higher D50-values obtained from SEM could represent a ‘worst case’ scenario for the RCS toxic potency of a gold dust sample.

This outcome supports the findings from Hegel et al. (2014) that differences can be expected, especially when the PSD metrics from two different methods are compared with one another, such as when SEM volume is compared with LLS volume.

The following study observations are made:

a) The SEM length and width measurements were made from a visual image and were used to calculate cross-sectional and spherical diameter and volume, where certain assumptions were made in the calculations. The aspect ratio of quartz (0.7) was used to calculate SEM ds (spherical diameter) for Arizona and gold mine dusts, which are mixtures of RCS and non-RCS particles.

b) LLS uses the refractive index of the material to derive the PSD, as the laser light is scattered by the particles. The LLS method measures the PSD in 3D as the particles move around in a liquid medium; in essence, the laser light shows the particles from all angles. The mineral composition, size, shape and PSD of the individual minerals contribute to the degree of variation in LLS results (Grubbs et al., 2021). The mineral dusts used in this study had a known concentration of RCS and for this reason, the refractive index for RCS in a suspension was used. The LLS method allowed for the adjustment of the refractive index to find the optimal refractive index for the dust being measured. In this study the adjustments were minor and their impacts on the PSD results were deemed negligible.

5.1.3 Objective 3: Estimation of the particle size of RCS from the SEM vs LLS regressions

The D50 PSD of RCS (SEM_{RCS}) in 12 samples with different mineral matrices, was estimated from the D50 PSD of all the dust particles (LLS_{Dust}) using the various regression equations and were then compared with the actual, measured D50 PSD of SEM_{RCS}. The estimated D50 PSD of SEM_{RCS} did not agree with the D50 PSD of the measured SEM_{RCS}.

The unknown gold mine dust samples were real workplace samples with an unknown mineral composition and PSD. It was anticipated that the PSD values might be variable because it was

sampled in a workplace and not prepared in a laboratory under controlled conditions like the NIST and Arizona dusts. Surprisingly, there was less variability in the estimated gold mine dust PSD parameters compared to those for NIST and Arizona.

The reason for this difference in actual values could also be related to the sample preparation for LLS compared to SEM. For SEM measurements the particles are measured as is, based on a visual image, and no sample preparation was required. If agglomerates are present, particles may partially overlap in such a way that it is difficult for the analyst to distinguish individual particles. On the other hand, the ultra-sonification step in LLS, to remove the dust particles from the membrane filter, may break down agglomerated particles that were sampled, hence the much smaller PSD seen from LLS compared to SEM. When a laboratory must estimate the PSD of RCS (SEM_{RCS}) from the PSD of dust (LLS_{Dust}), the impact of the sample handling and preparation will have to be quantified during the method validation process (SANAS, 2017). Grubbs et al. (2021) go further to suggest that the LLS and SEM instrument manufacturers may provide guidance on how the analysis methodology can be improved to obtain better sensitivity and consistency in the PSD results.

Assumptions in the conversion formulae could also explain differences between the actual values of the LLS and SEM results. Although these assumptions may give rise to differences in actual values, the observed trends should be similar (Hegel et al., 2014). Again, this contribution to the uncertainty of the PSD method will be quantified during a laboratory’s ISO 17025 method validation process to determine whether it is significant (ISO, 2017).

The SEM and LLS methods were applied to the same sample. Ideally, this would mean that for the purposes of comparing the two methods, the external factors that were involved in the collection of a sample should not be relevant. However, archived samples were used in this study without detailed information about the sampling conditions. The particle sizes of all the

samples were anticipated to be in the respirable range, i.e., less than 10 µm, but non-respirable particles (i.e. bigger particles or agglomerates) were found. Bigger particles in the sample could be a result of issues related to the sampling equipment itself. These issues might include the under-performance of the size-selective sampler (Stacey et al., 2013), incorrect sampling pump flow rate (ISO, 2022), and/or that the pump pulsation was out of specification (Lee et al., 2014). If risk assessments are conducted or RCS controls in the workplace are going to be implemented based on the PSD results, the contextual information of the sample must be carefully documented and closely controlled to assist the decision-making process. External factors may influence the quality of a respirable dust sample so that the measured PSD is not representative of what the mine employee was exposed to during the working shift.

For the gold mine dust, there could have been issues specific to the workplace, or the handling and transport of the sample to the analytical facility. For example, if the sample was not handled with care some of the dust particles may be dislodged, resulting in particles overlapping or agglomerating, which in turn had a negative impact on the SEM analysis results. Inaccurate PSD results may harm the implementation or adjustment of control measures to reduce the concentration of RCS-containing dust that mine employees are exposed to.

5.2 Study limitations

The study had the following limitations:

a) There are fundamental differences between the LLS and SEM methods. LLS does not provide a particle size measurement for each individual particle but provides a mathematically derived particle size distribution. By contrast, the SEM provides a particle size measurement for each individual particle and the aggregated results were

used determine the PSD. The limitation in this study was that only one PSD parameter i.e. the D50 (median) value could be used for comparison.

b) The characterisation of the mineral composition of the gold mine dust was not done and neither was the RCS mass concentration determined. SEM-EDS was only used to confirm that the particles that were measured, were particles with an elemental composition similar to SiO_2 (silicon dioxide).

c) The outcomes of this study relate only to the mineral dusts tested and cannot be extrapolated to other mineral dusts, such as coal dust. Similar PSD measurements using LLS and SEM will be required to assess if a favourable regression can be obtained on other mineral dusts.

Chapter 6: Conclusions and Recommendations

6.1 Introduction

Concluding remarks, recommendations and points to consider for future research are provided in this Chapter.

6.2 Conclusion

The particle size of RCS has been implicated in the toxicity of RCS-containing dust (Pollard, 2016). The aim of this study was to investigate the performance of an affordable, high-throughput method (LLS_{Dust}) to estimate the particle size of RCS in archived dust samples by comparing the results obtained by LLS_{Dust} with the results from SEM_{RCS}, considered to be the gold standard, an expensive, labour-intensive method.

The main finding of the study was that the measurement of the PSD of dust by LLS ($PSD_{LLS(Dust)}$) does not accurately represent but systematically underestimates the PSD of RCS by SEM ($PSD_{SEM(RCS)}$). Despite this disappointing outcome, it was possible to operationalise the SEM_{RCS} measurement to be very efficient, and it may not be necessary to estimate SEM_{RCS} from LLS, but to conduct direct SEM measurements.

6.3 Recommendations

The outcomes from this study lead to the following recommendations:

a) It is recommended that direct SEM measurements to determine the RCS particle size are routinely done instead of LLS.
b) It is recommended that colour-coding and mapping is used on SEM-EDS to identify, select and measure 100 RCS particles. This approach will enable the efficient and affordable routine analysis of RCS particle sizes in workplace samples and should be used in exposure assessments.

c) It is recommended that when similar regressions are looked for in future, the actual aspect ratio for the material in question is measured and used in the SEM calculations for cross-sectional and spherical diameter, and the volume.

d) Although the LLS method is not the preferred method, it is likely to be used in practice, and the method can be improved. It is recommended that the refractive index of a mixed mineral dust is determined and used in the measurement. Supplementary analysis to determine the composition of the mixture of dust (i.e. by x-ray diffraction) can be done and the refractive index can be obtained for known, individual minerals from literature. The refractive index can be estimated for the mineral dust mixture. The LLS software enables a further improvement of the refractive index for the analysis of the mixture of minerals in the dust.

e) When preparing regressions for use in practice, it is recommended that the regressions are robust and fit for purpose. Real-world samples may have specific characteristics, compositions or anomalies that require a non-linear regression model. Non-linear regression models may be better when regressions are prepared for predictive analysis for SEM from LLS, for a particular project, mineral matrix or a group of samples. Real-world samples may have specific characteristics, compositions or anomalies that require a non-linear regression model.

f) The combination of SEM and LLS may be useful to characterise workplace dusts. When SEM_{RCS} is estimated from LLS_{Dust}, it is important that the laboratory conducts a comprehensive method validation process and cross-examines the actual PSD values obtained from SEM and LLS. The actual differences between the two PSD metrics (e.g. LLS Vol *vs.* SEM dc) should follow a similar and consistent pattern that is useful

for predictive analysis. For example, Grubbs et al. (2021) evaluated the impact of each analytical metric that may contribute to the uncertainty associated with each PSD result.

g) It is recommended that the laboratory analyst has a good understanding of the type of information that the client requires and how the PSD information will be applied. When the PSD is used to implement or improve RCS-control measures, the selection of PSD metrics from LLS and SEM must be focused on the intended purpose. Typically, the laboratory will improve the calibration for specific PSD metrics (e.g. LLS Volume *vs.* SEM ds). At this stage, it is unclear which PSD metric will be the most suitable for a control measure (e.g. water-based sprays or filtration system).

6.4 Future Research

This study provides the basis for future research related to the measurement of the PSD of RCS in mineral dust mixtures. The following topics are suggested for future research:

a) In this study 100 RCS particles were measured but the SEM method can be operationalised for effort by determining the minimum number of RCS particles that should be measured using a sensitivity test and mathematical modelling. If the number of particles could be reduced the method could be further improved for efficiency and effort during routine analysis.

b) Future research should be undertaken on the impact on the SEM and LLS comparison of the mineral composition of the dust samples obtained from different workplaces.

c) Future research should investigate the contribution of the RCS particle size in relation to the improvement of dust-control measures to reduce worker exposure to RCS and the subsequent development of silicosis. The efficiency of controls is usually adjusted for the PSD of mixed dust particles and not for the PSD of RCS specifically (NIOSH,

2019, Animah et al., 2024). If the RCS particles are significantly different from the non-RCS dust particles, the controls must be adjusted to control both dust and RCS.

References

Animah, F., Keles, C., Reed, & W.R. et al. (2024) Effects of dust controls on respirable coal mine dust composition and particle sizes: Case studies on auxiliary scrubbers and canopy air curtain. *International Journal of Coal Science & Technology*, 11, 33. doi.org/10.1007/s40789-024-00688-8.

ASTM. (2014) *Standard test method for determining particle size distribution of alumina or quartz by laser light scattering*. ASTM C1070-01. West Conshohocken, PA: American Society for Testing and Materials International.

Bland, J.M. & Altman, D.G. (1995) Comparing methods of measurement: Why plotting difference against standard method is misleading. *Lancet*, 346(8982), 1085–7. doi.org/10.1016/s0140-6736(95)91748-9.

Brouwer, D.H. & Rees, D. (2020) Can the South African milestones for reducing exposure to respirable crystalline silica and silicosis be achieved and reliably monitored? *Frontiers in Public Health*, 8(107). doi.org/10.3389/fpubh.2020.00107.

Castranova, V. (2004) Signalling pathways controlling the production of inflammatory mediators in response to crystalline silica exposure: Role of reactive oxygen/nitrogen species. *Free Radical Biology and Medicine*, 37, 916–925.

Chubb, L. & Cauda, E.G. (2017) Characterizing particle size distributions of crystalline silica in gold mine dust. *Aerosol and Air Quality Research*, 17, 24–33. doi.org/10.4209/aaqr.2016.05.0179 .

Diez-Gil, C., Martinez, R., Ratera, I., Tárraga, A., Molina, P., & Veciana, J. (2008). Nanocomposite membranes as highly selective and sensitive mercury(II) detector. *Journal of Materials Chemistry.* 18. doi.org/10.1039/b800708j.

DME. (2006, October) 2006 Occupational Exposure Limits for Airborne Pollutants. *Government Gazette No. 29276.* Department of Minerals Energy Available from: https://www.gov.za/sites/default/files/gcis_document/201409/29276.pdf.

DMR. (2018, April) Guideline for the compilation of a mandatory code of practice for an occupational health programme (occupational hygiene and medical surveillance) on personal exposure to airborne pollutants. Department of Mineral Resources Available from: https://www.mhsc.org.za/sites/default/files/public/legislation_document/Airborne%20Pollutants%20Guideline_0.pdf [Accessed on 2024-11-11].

DMRE. (2023) Mine Health and Safety Inspectorate: Annual Report 2022/2023. Department of Mineral Resources and Energy. Available from: https://static.pmg.org.za/MHSI_Annual_Report_2022-2023_pdf.pdf [Accessed 02-09-2024].

DOL. (2006, 22 July) National Programme for the Elimination of Silicosis in South Africa. Occupational Health Southern Africa. Department of Labour Available from: https://www.occhealth.co.za/_assets/articles/162/677.pdf.

Dunn, O.J. (1961) Multiple comparisons among means. *Journal of the American Statistical Association*, 56, 54-64.

EPA. (2002, September) *Guidelines for the application of SEM/EDX analytical techniques to particulate matter samples.* EPA # 600/R-02/070. Environmental Protection Agency. Available from: https://nepis.epa.gov/Exe/ZyPURL.cgi?Dockey=P1005I40.txt. [Accessed 20-05-2018].

Fubini, B., Fenoglio, I., & Ceschino, R., et al. (2004) Relationship between the state of the surface of four commercial quartz flours and their biological activity in vitro and in vivo. *International Journal of Hygiene and Environmental Health*, 207:89–104.

Garbin, V, Volpe, G, Ferrari, E, Versluis, M, Cojoc, D, & Petrov, D. (2009) Mie scattering distinguishes the topological charge of an optical vortex: a homage to Gustav Mie. *New Journal of Physics*, 11(1).

Getman, M., Webber, J. & Bowser, S. (2017) An examination of MCE filter morphology and implications on preparation and analysis of air samples for asbestos, *Journal of Occupational and Environmental Hygiene*, 14(9), D140-D144.

Grubbs, J., Tsaknopoulos, K., & Massar, C., et al. (2021) Comparison of laser diffraction and image analysis techniques for particle size-shape characterization in additive manufacturing applications. *Powder Technology*, 391, 20–33. doi.org/10.1016/j.powtec.2021.06.003.

Hall, S., Stacey, P., & Pengelly, I., et al. (2022) Characterizing and comparing emissions of dust, respirable crystalline silica, and volatile organic compounds from natural and artificial stones. *Annals of Work Exposures and Health*, 66(2), 139–149.

Hebisch, R., Fricke, H.H., & Hahn, J-U., et al. (2005) Chapter 9 – Sampling and determining aerosols and their chemical components. In: Parlar, H. and Greim, H eds, *The MAK-Collection for occupational health and safety, Part III: Air monitoring Methods*, pp. 3–40. Weinheim: Wiley-VCH Verlag. doi.org/10.13140/2.1.4181.9202.

Hegel, C., Jones, C., & Cabrera, F., et al. (2014) Particle size characterization: Comparison of laser diffraction (LD) and scanning electron microscopy (SEM). *Acta Microscopica*, 23, 11–17.

Horiba Scientific. (2007) *Horiba laser scattering particle size distribution analyser. Partica LA-950V2* [Brochure]. Available from: http://www.horiba.com/fileadmin/uploads/ Scientific/Documents/PSA/LA950_V2_bro.pdf. [Accessed 20-05-2018].

Horiba Scientific. (2019) *A guidebook to particle size analysis*. Available from: https://static.horiba.com/fileadmin/Horiba/Products/Scientific/Particle_Characterization/Particle_Guidebook_2022.pdf [Accessed 30-03-2023].

HSE. (n.d.) Methods for determination of hazardous substances (MDHS) 101, 2nd Edition. Crystalline silica in respirable airborne dusts – Direct on-filter analyses by infrared spectroscopy and X-ray. Health and Safety Executive. Available from: https://www.hse.gov.uk/pubns/mdhs/pdfs/mdhs101.pdf [Accessed: 2024-11-07].

IARC. (2012) *Arsenic, metals, fibres, and dusts: IARC Monograph Vol. 100 C: A review of human carcinogens.* Lyon: International Agency for Research on Cancer.

ILO. (2021) *Exposure to hazardous chemicals at work and resulting health impacts: A global review*. Geneva: International Labour Office.

Illowsky, B. and Dean, S., 2013. Introductory Statistics 2e. OpenStax.

ISO. (1995) *Air quality – Particle size fraction definitions for health-related sampling*. Geneva: International Organization for Standardization.

ISO. (2011) *Microbeam analysis — Quantitative analysis using energy-dispersive spectrometry (EDS) for elements with an atomic number of 11 (Na) or above*. ISO 22309. Geneva: International Organization for Standardization.

ISO. (2016) *Workplace air — Terminology*. ISO 18158. Geneva: International Organization for Standardization.

ISO. (2017) *General requirements for the competence of testing and calibration laboratories.* ISO 17025. Geneva: International Organization for Standardization.

ISO. (2020) *Particle size analysis – Laser diffraction methods*. ISO 13320 Geneva: International Organization for Standardization.

ISO. (2022) *Workplace atmospheres—pumps for personal sampling of chemical and biological agents—requirements and test methods*. ISO 13137. Geneva: International Organization for Standardization.

Johann-Essex, V., Keles, C. & Sarver, E. (2017) A computer-controlled SEM-EDX routine for characterizing respirable coal mine dust. *Minerals,* 7(1), 15. doi.org/10.3390/min7010015.

Kawasaki, H. (2015) A mechanistic review of silica-induced inhalation toxicity. *Inhalation Toxicology* 27(8), 363–77. doi.org/10.3109/08958378.2015.1066905.

Keles, C. & Sarver, E. (2022) A Study of Respirable Silica in Underground Coal Mines: *Particle Characteristics. Minerals*, 12, 1555. doi.org/10.3390/min12121555.

Knight, D., Ehrlich, R., Fielding, K., et al. (2015) Trends in silicosis prevalence and the healthy worker effect among gold miners in South Africa: A prevalence study with follow up of employment status. *BioMed Central Public Health,* 15, 1258. doi.org/10.1186/s12889-015-2566-8.

Kruskal, W.H. & Wallis, W.A. (1952). Use of ranks in one-criterion variance analysis. *Journal of the American Statistical Association,* 47 (260), 583–621. doi.org/10.1080/01621459.1952.10483441.

Lee, E.G., Lee, L., & Möhlmann, C., et al. (2014) Evaluation of pump pulsation in respirable size-selective sampling: Part I. Pulsation measurements. *Annals of Occupational Hygiene,* 58(1), 60–73. doi.org/10.1093/annhyg/met047.

Mamphitha, D. (2022, October) Final – MHSC CEO presentation on 2014 milestones progress. *Proceedings of the 2022 OHS* Summit *Presentation at the 2022 Occupational*

Health and Safety Tripartite Summit. Mine Health and Safety Council. Available from: https://mhsc.org.za/2022/10/18/ohs-summit-2022-day-1-presentations/ [Accessed 01-05-2023].

Mann, H.B. & Whitney, D.R. (1947) On a test of whether one of two random variables is stochastically larger than the other. *Annals of Mathematical Statistics*, 18(1), 50-60.

Mecchia, M., Pretorius, C., Stacey, P., Mattenklott, M., & Incocciati, E. (2013) X-ray absorption effect in aerosol samples collected on filter media. In: Harper M., & Lee T. (eds), *Silica and Associated Respirable Mineral Particles*, STP 1565. West Conshohocken, PA: ASTM International, pp. 139–68.

MHSC. (2014) Every mine worker returning from work unharmed every day. Striving for zero harm. In: *2014 Occupational Health and Safety Summit Milestones* [Media release]. Mine Health and Safety Council. Available from: http://www.chamberofmines.org.za/industry-news/media-releases/2014/send/11-2014/41-2014-occupational-health-safety-summit-milestones [Accessed 26-02-2018].

National Institutes of Health (NIH), USA. (2018) *Download ImageJ* [Software]. Available from: https://imagej.nih.gov/ij/download.html [Accessed 25-02-2023].

NIOH. (2020) *Pathology division surveillance report 1/2022. Demographic data and disease rates for January to December 2020.* National Institute of Occupational Safety and Health. Available from: https://www.nioh.ac.za/wp-content/uploads/2023/04/Pathaut_Report_2020.pdf [Accessed 27-04-2023].

NIOH. (2021) *Pathology division surveillance report 1/2022. Demographic data and disease rates for January to December 2021*. National Institute of Occupational Safety and Health. Available from: https://www.nioh.ac.za/wp-content/uploads/2023/10/PATHAUT_Report_2021.pdf [Accessed 27-01-27].

NIOSH. (2002) *NIOSH hazard review: Health effects of occupational exposure to respirable crystalline silica*. National Institute for Occupational Safety and Health. DHHS (NIOSH) Publication No. 2002-129. OSHA-2010-0034-1110. Cincinnati, OH: US Department of Health and Human Services, Public Health Service, Centers for Disease Control and Prevention.

NIOSH. (2019, March). *Dust control handbook for industrial minerals mining and processing*. 2nd Edition. National Institute of Occupational Safety and Health, Centers for Disease Control and Prevention. Available from: https://www.cdc.gov/niosh/mining/UserFiles/works/pdfs/2019-124.pdf. [Accessed: 2022-06-21]

NIST. (1999) *Respirable alpha quartz*. National Institute of Standards and Technology. SRM 1878a. Gaithersburg, MD: US Department of Commerce.

National Metrology Institute of South Africa (NMISA) https://www.nmisa.org/Pages/About-Metrology.aspx [Accessed: 2022-06-21]

OSHA. (2016) *Occupational exposure to respirable crystalline silica – review of health effects literature and preliminary quantitative risk assessment*. OSHA-2010-0034.

Occupational Safety and Health Administration. Available from: https://www.regulations.gov/docket/OSHA-2010-0034. [Accessed: 2021-06-21]

Page, SJ. “Crystalline Silica Analysis: A Comparison of Calibration Materials and Recent Coal Mine Dust Size Distributions.” Journal of ASTM International 3, no. 1 (n.d.): JAI12236-. *https://doi.org/10.1520/JAI12236*.

Pavan, C. & Fubini, B. (2017) Unveiling the variability of “quartz hazard” in light of recent toxicological findings. *Chemical Research in Toxicology*, 30(1), 469–85. doi.org/10.1021/acs.chemrestox.6b00409.

Pollard, K.M. (2016) Silica, silicosis, and autoimmunity. *Frontiers Immunology*, 7, 97. doi.org/10.3389/!mmu.2016.00097.

Powder Technology. (2020) *Material safety data sheet of Arizona dust*. Available from: *https://www.powdertechnologyinc.com/wp-content/uploads/2023/12/SDS.Arizona-Test-Dust.20-May-2020-US-version.pdf [Accessed on: 2024-12-05]*

Pretorius, C.J. (2011a) Particle capturing performance of South African non-corrosive samplers. *Journal of the Mine Ventilation Society of South Africa*, 64(4), 8–13.

Pretorius, C.J. (2011b) The effect of size-selective samplers (cyclones) on XRD response. *Journal of the Mine Ventilation Society of South Africa*, 64(3), 8–12.

Qi, C., Echt, A. & Gressel, M.G. (2016) On the characterization of the generation rate and size-dependent crystalline silica content of the dust from cutting fiber cement siding. *Annals of Occupational Hygiene,* 60, 220–230.

Rees, D. & Murray, J. (2007) Silica, silicosis and tuberculosis. *International Journal of Tuberculosis and Lung Disease,* 11(5), 474–484.

Ross, A. and Willson, V.L. (2017) *Paired samples t-test: Basic and advanced statistical tests.* Rotterdam: Sense Publishers. doi: 10.1007/978-94-6351-086-8_4.

SANAS. (2017) *Criteria for validation of methods used by chemical laboratories in the coal, oil, petroleum, metals and minerals, food, pharmaceutical, water and related industries*. TR26-03. Johannesburg: South African National Accreditation System.

SANAS. (2020, January) *Schedule of accreditation for CSIR A&D Laboratory*. T0420. Johannesburg: South African National Accreditation System.

Sarver, E., Keles, C. & Rezaee, M. (2019) Beyond conventional metrics: Comprehensive characterization of respirable coal mine dust. *International Journal of Coal Geology,* 207, 84–95. doi.org/10.1016/j.coal.2019.03.015.

Sarver, E., Keles C., & Afrouz, S.G. (2021) Particle size and mineralogy distributions in respirable dust samples from 25 US underground coal mines. *International Journal of Coal Geology*, 247, Art 103851, doi.org/10.1016/j.coal.2021.103851.

Schneider, C., Rasband, W. & Eliceiri, K. (2012) NIH Image to ImageJ: 25 years of image analysis. *Nature Methods*, 9, 671–675. doi.org/10.1038/nmeth.2089

Sellaro, R., Sarver, E. & Baxter, D. (2015) A standard characterization methodology for respirable coal mine dust using SEM-EDX. *Resources*, 4(4), 939–957. doi.org/10.3390/resources4040939..=

Shapiro, S. S. & Wilk, M. B. (1965) An analysis of variance test for normality (complete samples), *Biometrika*, 52(3-4), 591–611. doi.org/10.1093/biomet/52.3-4.591.

Stacey P., Kauffer E., Moulut J.C., Dion C., Beauparlant M. & Fernandez P. (2009) An international comparison of the crystallinity of calibration materials for the analysis of respirable α-quartz using x-ray diffraction and a comparison with results from the infrared KBr disc method. *Annals of Occupational Hygiene*, 53, 639–649.

Stacey, P., Mecchia, M. & Verpaele, S., et al. (2013) Differences between samplers for respirable dust and the analysis of quartz—An international study. Silica and associated respirable mineral particles. In: Harper, M. & Lee, T. (eds), *Proceedings of the ASTM Second Symposium on Silica and Associated Respirable Mineral Particles on October 25–26, Atlanta*: pp. 73–102. doi.org/10.1520/ STP156520120188.

Steenland, K., Mannetje, A., & Boffetta, P., et al. (2001). Pooled exposure-response and risk assessment for lung cancer in 10 cohorts of silica-exposed workers: An IARC multi-centric study. OSHA-2010-0034-0452. *Cancer Causes Control,* 12, 773–784.

Wallace, W.E., Keane, M.J., & Harrison, J.C., et al. (1996) Surface properties of silica in mixed dusts. OSHA-2010-0034-1132. In: Castranova, V., Vallyathan, V. & Wallace, W.E. (eds), *Silica and silica-induced lung diseases*: 107–117. Boca Raton, FL: CRC Press.

Walock, M. (2012) *Nanocomposite coatings based on quaternary metal-nitrogen and nanocarbon systems.* University of Alabama (doctorate).

WHO. (1999, August) Chapter 1 – Dust: Definitions and concepts. In: *Hazard prevention and control in the work environment: Airborne dust*. WHO/SDE/OEH/99.14. Geneva: World Health Organization.

Appendices

Appendix 1: Senate Plagiarism Policy

UNIVERSITY OF THE WITWATERSRAND, JOHANNESBURG

FACULTY OF HEALTH SCIENCES

PLAGIARISM DECLARATION TO BE SIGNED BY ALL HIGHER DEGREE STUDENTS

SENATE PLAGIARISM POLICY: APPENDIX ONE

I Cecilia Johanna Pretorius (Student number: 497084) am a student registered for the degree of MSc Medicine Exposure Science in the academic year 2025.

I hereby declare the following:

- I am aware that plagiarism (the use of someone else’s work without their permission and/or without acknowledging the original source) is wrong.
- I confirm that the work submitted for assessment for the above degree is my own unaided work except where I have explicitly indicated otherwise.
- I have followed the required conventions in referencing the thoughts and ideas of others.
- I understand that the University of the Witwatersrand may take disciplinary action against me if there is a belief that this is not my own unaided work or that I have failed to acknowledge the source of the ideas or words in my writing.
- I have included as an appendix a report from “Turnitin” (or other approved plagiarism detection) software indicating the level of plagiarism in my research document.

Signature: _____ Date: 03/03/2025

Appendix 2: Ethics Clearance

UNIVERSITY OF THE WITWATERSRAND, JOHANNESBURG

HUMAN RESEARCH ETHICS COMMITTEE (NON-MEDICAL)

Registration number: REC-101114-044

16 July 2020

Re: Mrs. Cecilia Pretorius (497084)
Waiver letter number: HRECNMW20/07/06

To whom it may concern,

Mrs. Pretorius is currently registered as a Masters student at the School of Public Health at the University of the Witwatersrand, Johannesburg. This letter is to confirm that, at the time of writing, Mrs. Pretorius does not need ethical clearance for her Masters study entitled *‘The estimation of the particle size of respirable crystalline silica from the particle size distribution measurement of archived dust samples’*. This decision has been reached based upon a description of the project supplied by Mrs. Pretorius to the University Human Research Ethics Committee (Non-Medical), which has been evaluated by the Chairs and Deputy Chairs. If, however, Mrs. Pretorius changes the methods of data collection and analysis for this study, this decision may no longer be valid. If such changes take place, this should be communicated to the University Human Research Ethics Committee (Non-Medical) as soon as possible. This waiver letter is valid until 15 July 2023.

Please feel free to contact me should you require any further information.

Thank you.

Yours sincerely,
S Schoeman

Shaun Schoeman (Administrative Officer)
Solomon Mahlangu House, 10th Floor, Room 10004, Jorissen Street, Braamfontein, Johannesburg
Private Bag 3, Wits 2050
T + 27(0)11 717 1408 | **E** Shaun.Schoeman@wits.ac.za | hrec-medical.researchoffice@wits.ac.za
www.wits.ac.za/research/about-our-research/ethics-and-research-integrity/

Appendix 3: Turnitin Report

04/12/2024, 11:46 Turnitin - Originality Report - Cecilia J. Pretorius Thesis Rev 1_2024-12-04....

Turnitin Originality Report

Document Viewer

Supervisor 5th December 2024

Processed on: 04-Dec-2024 11:34 AM SAST
ID: 2540322099
Word Count: 22624
Submitted: 1

Cecilia J. Pretorius Thesis Rev 1_2024-12-04....
By Cecilia Pretorius

Similarity Index	Similarity by Source	
9%	Internet Sources:	7%
	Publications:	6%
	Student Papers:	1%

include quoted | include bibliography | excluding matches < 8 words | mode: quickview (classic) report | print | download

<1% match ()
Kamanzi, Kankindi Conchita, von Holdt, Johanna, Jacobs, Muazzam, "Characterising the potential health risks associated with coal dust", Department of Chemical Engineering, 2023

<1% match ()
Marasabessy, Ahmad, "Lactose hydrolysis by immobilized whole cells of K. lactis CBS 2357 : a thesis presented in partial fulfilment of the requirements for the degree of Master of Technology in Bioprocess Engineering at Massey University", Massey University, 1999

<1% match ()
Hedges, Kevin, "Assessment and control of respirable crystalline silica in quarries and dimension stone mines", 'American Psychological Association (APA)', 2016

<1% match ()
Mametja, Thapelo Given, "An uncertainty budget for the precursor Watt balance for South Africa", Department of Physics, 2020

<1% match ()
Healy, Catherine, "Respirable Crystalline Silica Exposures among Stoneworkers involved in Stone Restoration Work", 2014

<1% match ()
Paule, Cleoper, Paule, Cleoper, "Molecular bases underlying the sensitivity of the capsaicin receptor: TRPV1", Medicine: Sensory Processing Group, 2010

<1% match ()
Idamokoro, Mare, "Physiological traits, anthropometric characteristics and motor development of rural children in Nkonkobe Municipality, South Africa", Faculty of Health Sciences, 2018

<1% match ()
Swanepoel, Andrew Johnstone, "Exposure to respirable crystalline silica in central South Africa farm workers", 2013

<1% match (Internet from 04-Apr-2016)
http://www.mdpi.com

<1% match (Internet from 28-Dec-2023)
https://WWW.MDPI.COM/2075-163X/13/4/581

<1% match (Internet from 24-Jun-2024)
https://www.mdpi.com/2073-4360/16/7/913

<1% match (Internet from 06-May-2024)
https://wiredspace.wits.ac.za/server/api/core/bitstreams/4126f1a2-ce3b-472d-90af-3b60265b9d3e/content

<1% match (Internet from 10-May-2024)
https://wiredspace.wits.ac.za/server/api/core/bitstreams/fe5134ac-c198-4aed-904a-c86e5b3dde5d/content

<1% match (Internet from 07-May-2024)
https://wiredspace.wits.ac.za/server/api/core/bitstreams/51a66ec2-f3d2-426f-9d27-b4bbb290bdbb/content

<1% match (Internet from 06-May-2024)
https://wiredspace.wits.ac.za/server/api/core/bitstreams/35d1023f-63f0-43f6-8e31-ab27209ae693/content

<1% match (Internet from 08-May-2024)
https://wiredspace.wits.ac.za/server/api/core/bitstreams/98e9059a-bc85-4e6a-8958-c97ae013e26f/content

<1% match (Internet from 10-Jan-2023)
https://core.ac.uk/download/pdf/148364846.pdf

<1% match (Internet from 03-Apr-2022)
https://core.ac.uk/download/232598533.pdf

<1% match (Internet from 21-Oct-2024)
https://core.ac.uk/download/188772984.pdf

<1% match (Internet from 21-Mar-2022)
https://core.ac.uk/download/231801983.pdf

<1% match (Internet from 07-Dec-2022)
https://scholar.sun.ac.za/bitstream/handle/10019.1/71635/bester_investigation_2012.pdf.txt?sequence=3

<1% match (Internet from 21-Mar-2023)
http://scholar.sun.ac.za

<1% match (student papers from 03-Apr-2022)

https://api.turnitin.com/newreport_classic.asp?lang=en_us&oid=2540322099&ft=1&bypass_cv=1 1/24

Appendix 4: Objective 1 results for Arizona and gold mine dust

A4.1. Operationalise particle sizing on Arizona ultra-fine dust (mixture)

The line sizing tool and subsequent calculations were applied to the particles of a well-defined mixture of dust: Arizona dust, which consists of silica and non-silica particles.

It should be noted that the manual measurements were taken on RCS particles only, as shown in Figure A4.1. The manual measurement of silica particles was in line with the aim of the study, which was to determine the particle size of RCS.

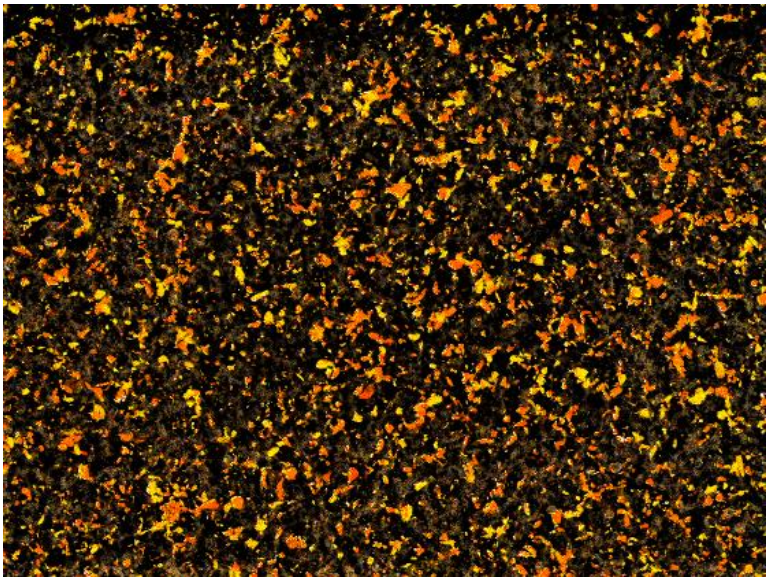

Figure A4.1: Manual measurements were taken on RCS particles only (yellow particles)

Figure A4.2 shows the D10, D50 and D90 parameters of the RCS particle size results that were taken on 112 particles on five areas of one filter with Arizona dust.

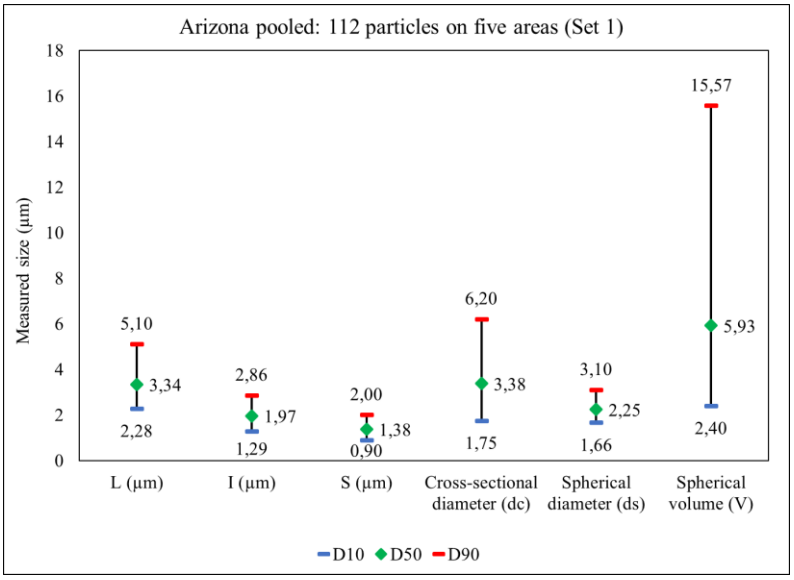

Figure A4.2: Particle size results on five areas of one filter with Arizona dust

A comparison between the spherical diameter (ds), cross-sectional diameter (dc) and volume (V) of the particle size results in each area with the pooled results (n=112) as shown in Figure A4.3, Figure A4.4 and Figure A4.5. Area S2A3 shows a larger variation than the other areas, possibly as a result of the poorer quality of the SEM image. When S2A3 was excluded, no significant differences were found between the cross-sectional diameter of the four remaining areas and the pooled measurements (ANOVA $p = 0.46$). The same outcome was found for the spherical diameter ($p = 0.33$) and the volume ($p = 0.66$).

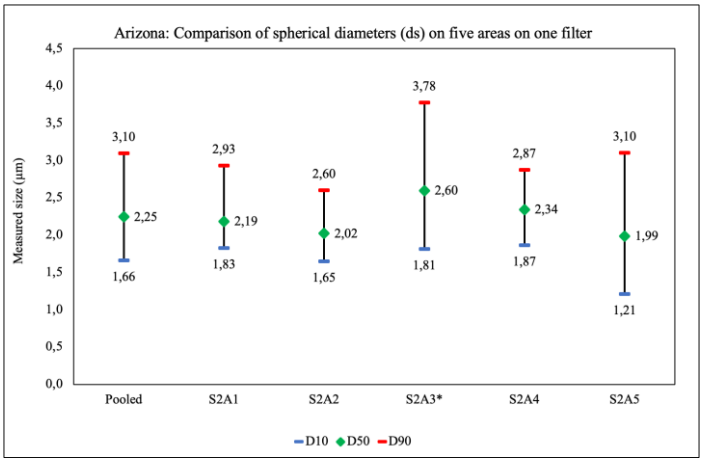

Figure A4.3: Comparison of the spherical diameter (ds) for each area with the pooled results in Arizona dust

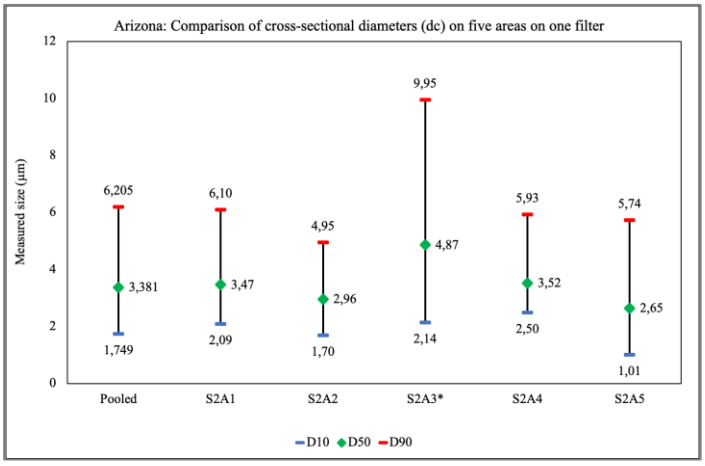

Figure A4.4: Comparison of the cross-sectional diameter (dc) for each area with the pooled results in Arizona dust

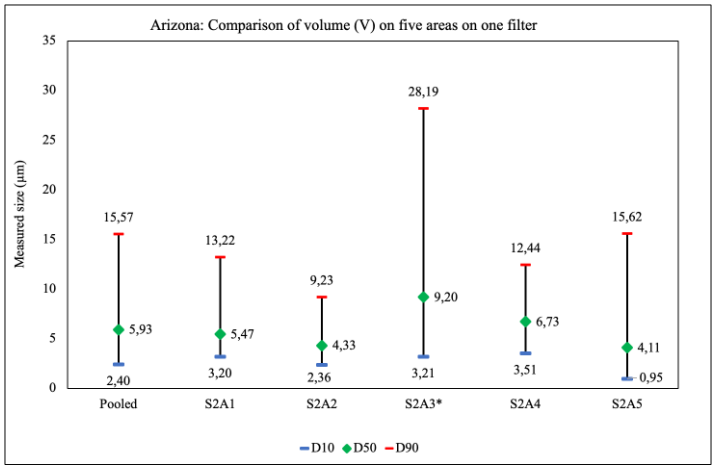

Figure A4.5: Comparison of the volume (V) for each area with the pooled results in Arizona dust

Table A4.1 shows a comparison of the RCS particle size results that were taken of the Arizona dust. The material safety data sheet (MSDS) for the Arizona dust shows that the D50 is between 2.75 and 5.50 µm, as determined using LLS. The particle size results (dc, ds and V) compare well with the MSDS.

Table A4.1: Comparison of the RCS particle size results of the Arizona dust

PSD	Cross-sectional diameter (dc)	Spherical diameter (ds)	Spherical volume (V)
percentiles	µm	µm	µm
D10	1.75	1.66	2.40
D50	3.38	2.25	5.93
D90	6.20	3.10	15.57

A4.2. Operationalise particle sizing on an unknown gold mine dust sample

Five areas were selected on the SEM specimen taken from the gold mine dust sample to determine the particle size of RCS particles. The length and width of a minimum of 20 RCS particles were measured in each of the five areas. A total of 170 RCS particles were measured using the line tool and the additional particle sizes were calculated from the line measurements. The D10, D50 and D90 data points were pooled and are shown in Figure A4.6.

The spherical volume had the widest range of particle size results, but the rest of the results compared well with one another.

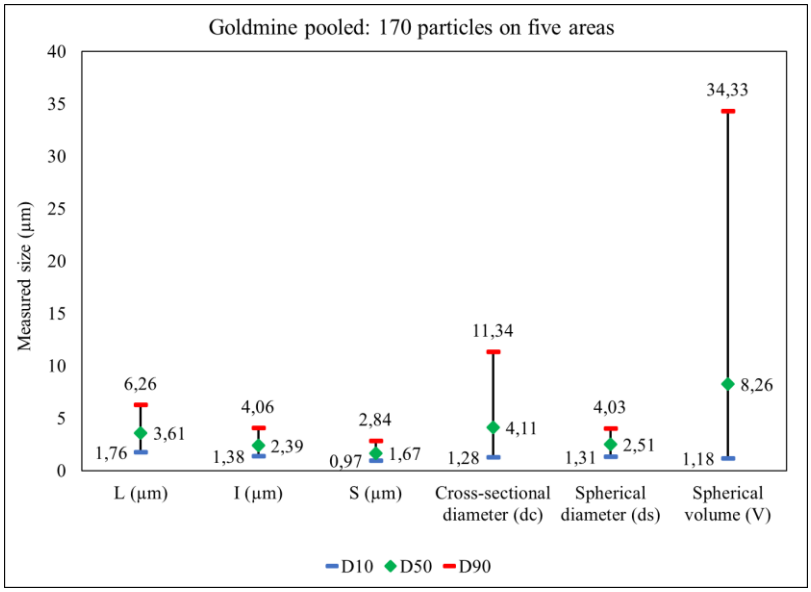

Figure A4.6: RCS particle size results on a gold mine dust sample

The comparison between the RCS particle size results of each area, with the results of all the RCS particles (n=170) in the gold mine dust sample, are shown in Figure A4.7, Figure A4.8 and Figure A4.9. Only the spherical diameter (ds), cross-sectional diameter (dc) and volume (V) of the RCS particles are shown in these figures.

The RCS particle size results on the individual areas compared well with the pooled results, which indicated that the dust distribution on the membrane filter was sufficiently homogenous for the SEM method.

The spherical diameter (ds) and cross-sectional diameter (dc) results showed promise because the sizes would be anticipated from real-world, personal-exposure samples with a size range of less than ± 10 µm. The size range of the spherical volume, however, was much larger than the spherical diameter (ds) and cross-sectional diameter (dc). The reason for this might be that the volume is calculated from the line measurements, with the assumption that the RCS particles are perfect spheres.

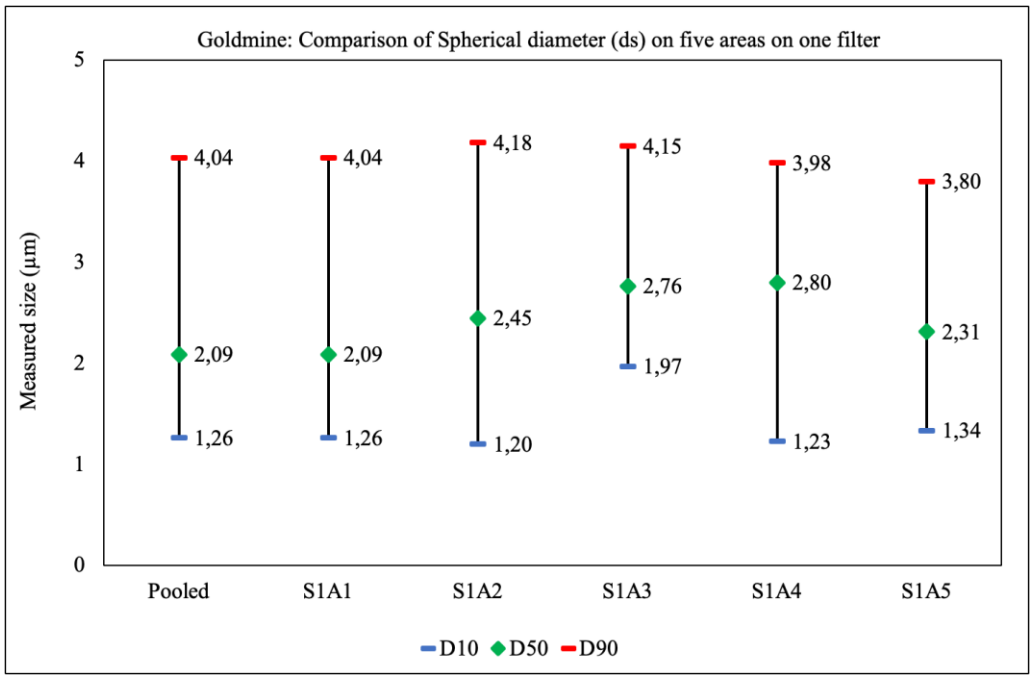

Figure A4.7: Comparison of the spherical diameter (ds) for each area with the pooled results in gold mine dust

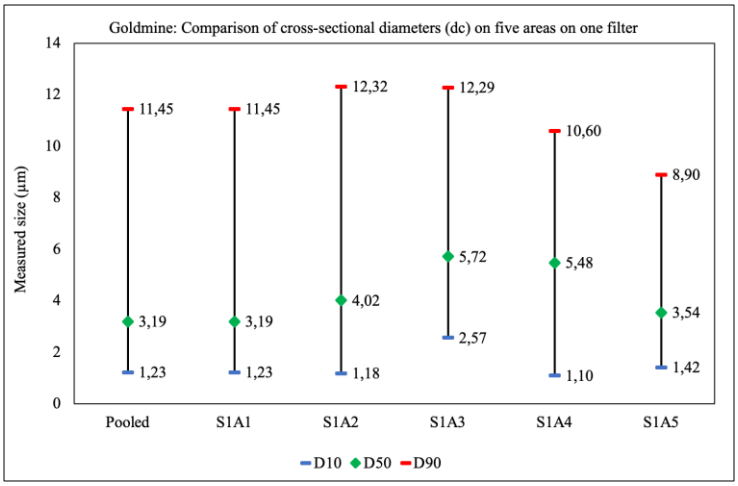

Figure A4.8: Comparison of the cross-sectional diameter (dc) for each area with the pooled results in gold mine dust

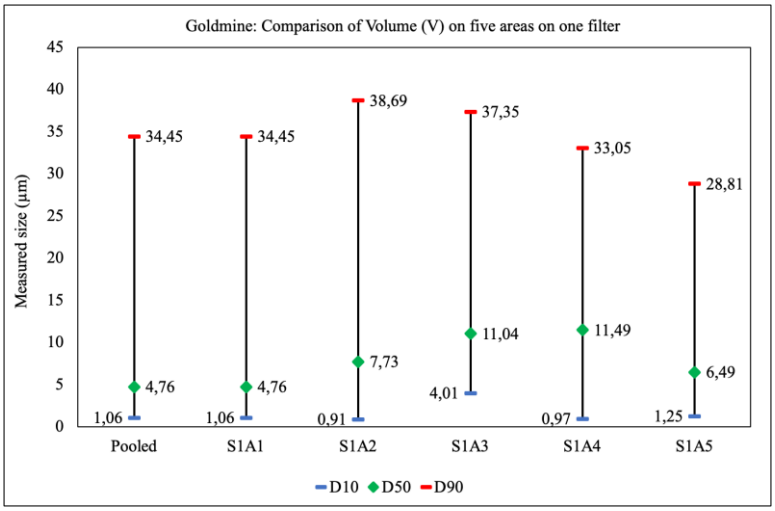

Figure A4.9: Comparison of the volume (V) for each area with the pooled results in gold mine dust

A4.3. Operationalise particle selection in Arizona with the additional particle properties

The cross-sectional diameter (dc), spherical diameter (ds) and volume (V) of the same RCS particles were mathematically derived from the length measurements. These RCS particle size results were expressed in terms of the PSD parameters (D10, D30, D50, D70 and D90). For ease of comparison the results are shown in Table A4.2, Table A4.3 and Table A4.4.

Table A4.2: PSD parameters for Arizona Group 1 (n=112)

PSD	Length	Width	Cross-sectional diameter	Spherical diameter	Spherical volume
Parameters	L (µm)	W (µm)	dc (µm)	ds (µm)	V (μm^3)
D10	2.28	1.29	1.75	1.66	2.40
D30	3.01	1.69	2.62	1.98	4.07
D50	3.34	1.97	3.38	2.25	5.93
D70	3.94	2.37	4.23	2.51	8.31
D90	5.10	2.86	6.20	3.10	15.57

Table A4.3: PSD parameters for Arizona Group 2 (n=111)

PSD	Length	Width	Cross-sectional diameter	Spherical diameter	Spherical volume
Parameters	L (µm)	W (µm)	dc (µm)	ds (µm)	V (μm^3)
D10	2.25	1.29	1.86	1.65	2.36
D30	2.79	1.71	2.41	1.89	3.51
D50	3.17	1.99	3.02	2.09	4.79
D70	3.65	2.27	3.80	2.40	7.28
D90	4.61	2.85	5.58	2.94	13.28

Table A4.4: PSD parameters for Arizona Group 3 (n=107)

PSD	Length	Width	Cross-sectional diameter	Spherical diameter	Spherical volume
Parameters	L (µm)	W (µm)	dc (µm)	ds (µm)	V (μm^3)
D10	1.72	1.36	1.41	1.42	1.49
D30	2.40	1.73	2.16	1.72	2.66
D50	2.76	2.05	3.02	2.03	4.36
D70	3.16	2.43	3.76	2.23	5.78
D90	4.28	3.00	5.01	2.64	9.64